Progress in Nuclear Energy 60 (2012) 89–116

Contents lists available at SciVerse ScienceDirect

Progress in Nuclear Energy

journal homepage: www.elsevier.com/locate/pnucene

Fusion energy conversion in magnetically confined plasma reactors

Flavio Dobran*

Hofstra University, Department of Engineering, Weed Hall, Hempstead, NY 11549, USA

ARTICLE INFO

Article history:
Received 11 November 2011
Received in revised form
24 May 2012
Accepted 29 May 2012

Keywords:
Fusion energy
Energy conversion
Heat transfer
Nuclear reactors
Liquid metals
Molten salts

ABSTRACT

One of the most pressing problems of this century is to solve the energy supply problem and in particular the development of fusion energy technology. Fusion powers the Sun and stars, but on Earth is difficult to achieve in a controlled manner. The International Thermonuclear Experimental Reactor (ITER) is the most technologically advanced machine where net energy from fusion is envisaged to be produced. But this will not be easy, since there are still open issues of plasma confinement, reactor materials, fuel supply, and heat removal. Efficient conversion of fusion energy into the thermal energy in a thermonuclear reactor is, therefore, of great technological relevance and in this paper the energy conversion in magnetically confined plasma reactors is addressed. The chamber wall surrounding the plasma is built from the plasma facing components and from the blanket and divertor modules where the fusion energy is converted into the thermal energy, tritium is produced, and the external components of the chamber are shielded from radiation. The useful materials for building the chamber wall components are low neutron activation steels, refractory metal alloys, and carbon fibre and silicon carbide reinforced composites. The suitable coolants of these components are high pressure helium gas and lithium-based liquid metals and molten salts, where the latter can also serve as tritium breeders. Some of these components will be tested in ITER and eventually may be employed for building demonstration fusion power plants envisaged to become operational during the second half of this century. High performance fusion energy conversion concepts being investigated include: Solid and liquid breeder blankets, separately cooled blankets and tritium breeders, high velocity helium jets for cooling plasma facing components, liquid metals flowing along the solid and through the porous metal walls facing the plasma, liquid metals and molten salts flowing through electrically insulated and non-insulated channels of blankets, and liquid metal heat pipes incorporated into the blankets and divertors for augmenting heat removal and achieving high thermal energy conversion efficiencies. The current fusion-to-thermal energy conversion technologies are, however, in an early stage of development and require reduced-activation, long life operation at high temperatures, resistance to plasma disruptions, and low fusion fuel retention materials, and innovative tritium breeding and heat removal concepts for building simple, reliable, safe, and efficient fusion energy technology.

1. Introduction

Fusion powers the Sun and stars and if we can reproduce it controllably on Earth and develop it commercially we could solve our energy problem. About 14 TW of power is used today by the world's population of seven billion people and this use is projected to more than double by 2050 when the additional two billion people will populate the planet (UNDESA, 2008; EIA, 2010). Most of the energy is used by the developed countries and the largest energy consumers are also the largest energy producers and exporters. About 85% of our energy needs are being supplied by fossil fuels (oil, gas, coal) and if this practice continues these fuels will be rapidly depleted during this century. The carbon emissions will continue to warm the atmosphere, produce costly global warming mitigation actions, and possibly produce unprecedented climate change effects (IPCC, 2007a,b; Dobran, 2010). Long-term security from the scarcity of energy sources, limits imposed on greenhouse gas emissions, and low risks of accidents associated with energy production are driving toward the development of alternative energy sources that are renewable on the long-term basis. The fusion energy is one of such alternatives.

Significant progress has been made in recent decades to develop renewable energy technologies by harnessing the solar energy directly (photovoltaics) or indirectly (solar panels and

* Tel.: +1 6314440212.
E-mail addresses: dobran@westnet.com, flavio.dobran@hofstra.edu.

0149-1970/$ – see front matter © 2012 Elsevier Ltd. All rights reserved.
doi:10.1016/j.pnucene.2012.05.008

concentrators, wind, biomass, hydro), but producing most of our energy needs with these technologies (that today amount to less than 10%) is difficult due to the low energy densities and efficiencies realized in solar collectors, intermittency of sunshine availability, inadequacy of electrical transmission grids, environmental constraints, and unfavorable economic incentives. Only about 7% of our electrical energy needs are today produced from 437 nuclear fission reactors, but the limited amounts of fissile materials available and low public acceptance of this technology are not becoming attractive enough to increase this capacity during this and the following centuries. The enormous amount of energy released from the fusion of light nuclei of deuterium, tritium, and helium offers the possibility of developing an inexhaustible energy source, but some of the scientific and technological problems associated with the harnessing on Earth of this energy source have not yet been completely worked out. To place the fusion energy in perspective, the annual fuel consumption of a 1000 MWe power plant requires about 3 million tonnes of coal, or 2 million tonnes of oil, or 30 tonnes of UO_2, or 100 kg of deuterium and 150 kg of tritium (Ongena and Van Oost, 2006). India and China alone are planning to increase their energy capacities in the next decades by over 2000 GWy, with half of the power plants burning coal and emitting over 10 GT/y of CO_2 into the atmosphere. The development of commercial fusion energy technology remains, therefore, an important goal of the developed nations (EUP, 2003; NAP, 2003), with this development being dictated by the availability and price of fossil fuels, environmental constraints, cost of alternative energy sources, and public acceptance (Dobran, 2011).

The controlled extraction of energy from nuclear fusion and its commercialization is a complex scientific and technological undertaking. Fusion of hydrogen and helium within the Sun takes place because the nuclei are brought close together by the intense pressure and temperature produced by gravity, but on Earth such an intense gravity is not available and alternate schemes are necessary to bring these nuclei together so that they can interact by the strong nuclear force that bounds the protons and neutrons together. One scheme employs large magnetic fields (magnetic confinement) which confine the charged isotopes of hydrogen for a sufficient time and at a high density and temperature to allow them to interact. The devices that employ this technology are the toruses (tokamaks, stellarators, multipoles), magnetic mirrors, and pinches. Another scheme employs the inertial confinement, whereby intense lasers or ion beams are used to direct energy on small pellets of fuel which through implosion produce the necessary fusion ignition condition. And in an electrostatic confinement the electric fields are used to bring the positively charged ions together (Gross, 1984; Harms et al., 2000). The development of fusion energy technology depends on the solutions of such problems as plasma heating and confinement, fuel supply, compatibility of plasma ions and neutrons with the surrounding chamber wall materials, heat removal and fuel breeding in the blanket of the reactor, removal of fusion products from the plasma through the divertor, radiation safety, public acceptance, etc. The efficiency of fusion-to-thermal energy conversion depends on the manner of achieving the best compromise between the plasma requirements, coolants, and tritium breeders with the materials employed to build the chamber wall of the reactor. The design of fusion reactors is therefore an extremely challenging technological problem and in this paper we will only address the energy conversion issues and concepts associated with tokamaks, because these machines are currently the most developed and envisaged to mature into the first generation demonstration reactors (DEMOs). Some energy conversion issues associated with the inertial confinement fusion reactors are different from the magnetically confined plasma reactors, but these will not be elaborated in this paper.

The magnetic and inertial confinement fusion reactor concepts are summarized in Section 2. This serves the purpose, in the following section, for assessing in magnetically confined plasma reactors the magnitudes and effects of heat and neutron fluxes on the materials of plasma facing components and reactor chamber wall blankets and divertors, coolants and heat removal concepts employed to convert the fusion energy into the thermal energy, and liquid and solid breeders used to produce tritium to fuel the reactors. Section 4 concludes with the prospects of developing a viable magnetic confinement plasma fusion energy conversion technology.

2. Magnetic and inertial confinement fusion reactors

2.1. Fusion reactions

The essential condition for fusion is the requirement that the nuclei of reacting species overcome their electrostatic Coulomb repulsion and thus become influenced by the strong nuclear force that binds neutrons and protons together. The fusion reaction most easily achieved in the laboratory is the deuterium–tritium (DT) reaction, because this requires deuterons (D = p,n) with less than 0.5 MeV of energy to strike tritons (T = p,2n). This reaction produces 17.58 MeV of energy, where a 14.06 MeV neutron and a 3.52 MeV helium nucleus (α = 2p,2n) are produced. This is the energy multiplication of 35 and thus the great interest in developing fusion energy technology. Another accessible fusion reaction is the DD reaction, which produces a proton and a triton in one branch and releases 4.1 MeV of energy, and a neutron and a helium-3 nucleus (h = 2p,n) in the second branch with the release of 3.2 MeV of energy. This reaction requires higher energies of nuclei for ignition than the DT reaction, but is more advantageous in terms of safety because it produces lower energy neutrons and thus causes considerably less damage to the reactor wall materials. A fusion reaction that produces no neutrons is the Dh reaction, which produces a proton and a helium nucleus with energies of 18.3 MeV (Harms et al., 2000). Advanced fusion cycles based on DD and Dh reactions offer some clear advantages over other cycles (Santarius et al., 1998), but their technologies are not sufficiently developed today to warrant further discussion in this paper.

The DT reaction is, therefore, of the immediate interest for developing the first generation fusion power plants, but its drawback is the lack of naturally occurring tritium fuel here on Earth. Lithium is, however, abundant and two of its isotopes ^{6}Li and ^{7}Li readily react with fusion neutrons of the DT fusion reaction and produce tritium, helium nucleus, and neutrons as the reaction products. Lithium surrounding the plasma and/or being a part of the reactor chamber coolant can be used for tritium breeding in first generation fusion power plants, and this is why the efficiency of energy conversion in a thermonuclear reactor depends on the choice of reactor chamber wall materials, coolants, and fusion fuel. A typical configuration of plasma, plasma facing first wall, tritium breeding and heat removal blanket, radiation shield, and other reactor components (vacuum vessel, magnets used in magnetic confinement) is illustrated in Fig. 1. The first wall is the protective armor of the blanket and can be built as a separate unit or integrally incorporated into the blanket. The neutrons are not confined within the plasma volume and interact with the reactor chamber wall materials where they heat the blanket, produce atomic displacements, and cause transmutations in these materials that render the first wall and blanket radioactive. Energy from the DT fusion reaction carried by the ions (alpha particles) and electrons is used for heating of plasma, some is deposited within the blanket from the loss of plasma confinement, while the rest is diverted to the divertor. The divertor serves the purpose of an exhaust pipe where

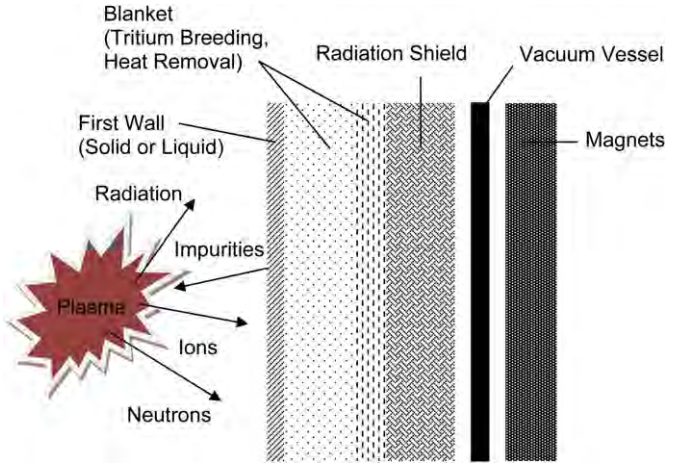

Fig. 1. The chamber wall of a magnetically confined plasma fusion reactor consists of a plasma facing first wall, blanket for tritium breeding and fusion energy removal, and shield for radiation protection. The vacuum vessel also acts as a shield and separates plasma from the external environment. The magnets are placed on the outside of the blanket and vacuum vessel for protection against radiation and easy maintenance.

the fusion ions, unburnt fuel, and impurities from the interaction of plasma with chamber wall materials are removed from the reactor. These exhaust products are sometimes referred to as the 'plasma ash'.

The power produced from fusion is proportional to ion density, reaction rate, energy released per fusion event (17.6 MeV for DT reaction), and reactor volume. The reaction rate is in turn proportional to the fuel type and ion temperature, and a self-sustaining (breakeven) fusion condition exists when the fusion energy released balances the energy losses from radiation and particles. The breakeven condition for DT reaction requires ion temperatures of about 12 keV (about 150 million K) and the product of ion density and confinement time ($n_i\tau_E$) of 10^{20} $m^{-3}s$. The DD reaction requires temperatures in excess of 150 million K and almost two orders of magnitude higher $n_i\tau_E$ (Gross, 1984). Since the fusion power in a magnetically confined plasma reactor is proportional to plasma pressure and magnetic field it is important to maximize these parameters.

2.2. Fusion reactor configurations

Tokamak is a closed magnetic field configuration system where the field lines used to confine the plasma at about 150 million K do not enter or leave the plasma confinement region. Some of the energy contained in the charged reaction products is diverted into the divertor through the open magnetic field lines residing on the outside of the plasma volume. The energy carried by fusion neutrons cannot be confined by the magnetic field; they deposit their energies within the blanket of the reactor from where the heat must be removed by suitable coolants and transferred to external heat exchange circuits to produce electricity or used as heat for process industries. The simplest of such configurations is a torus which employs several configurations of magnetic fields to stabilize the plasma against leaving the reaction volume and interacting with the surrounding chamber walls where it is rapidly cooled and can compromise the integrity of the reactor. In the tokamak configuration (Fig. 2), plasma is confined within the torus by the torodial, poloidal, and vertical stabilization magnetic fields supplied by the superconducting coils placed on the outside of the vacuum vessel. The current flowing through the (toroidal) coils wound around the vacuum vessel generates a strong steady-state toroidal magnetic field. The outer poloidal field coils are used to stabilize the magnetic field in the plasma. The inner field coils (central solenoid) produce a strong toroidal current for ohmic heating of plasma and a poloidal magnetic field. Heating by the current is, however, insufficient during the startup of the machine and additional heating of plasma with neutral particle injections or radiofrequency waves is necessary to produce a burning plasma or net fusion power output. The tokamaks thus operate in a pulsed mode, in contrast to the stellarators which are steady-state devices. The currents for heating plasmas in stellarators are generated in external conductors and not within the plasmas, but their designs are more complicated and less developed than those of tokamaks (Harms et al., 2000). Tokamak and stellarator experiments and

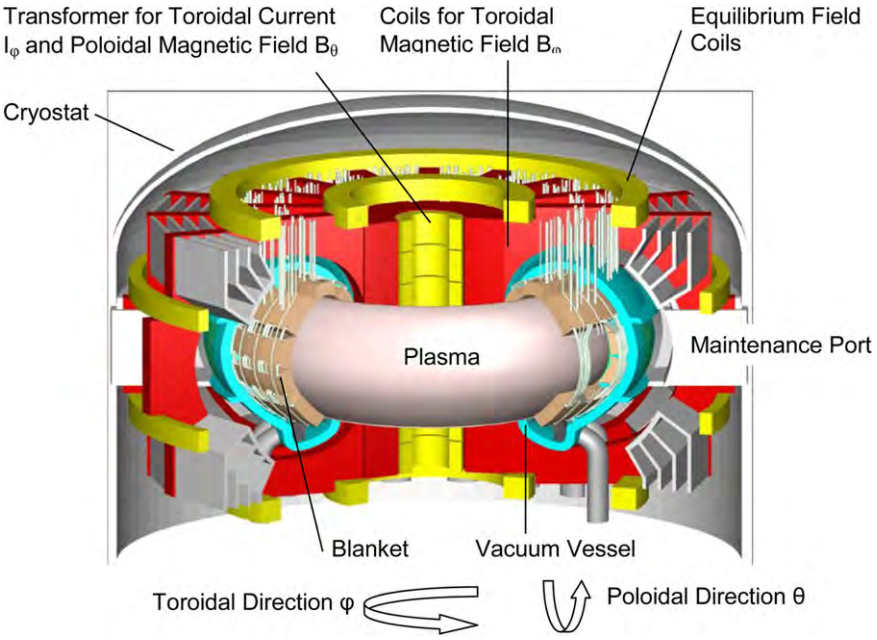

Fig. 2. Configuration of components in a tokamak. Courtesy of JAEA DEMO design.

conceptual studies are being conducted in China, EU, India, Japan, Russia, South Korea, and the United States. The Joint European Torus (JET) is the largest of these machines and it recently produced 16 MW of fusion energy (U.S. ARIES et al., 2005).

There are several ways of separating the plasma from the external environment and the topology illustrated in Fig. 2 has the following functions. It provides a high vacuum for maintaining the necessary plasma conditions; supports in-vessel components (blanket, divertor, radiation shields) and their resultant loads; provides access to the plasma through the ports for diagnostics and heating systems; allows for inlet and outlet manifolds for coolant and tritium recovery; provides a conductive shell for plasma stabilization; participates in the shielding against neutrons; allows for the decay heat removal in the event of a loss of the active coolant system; and because of the vacuum vessel's double-wall design it acts as a primary barrier against the release of radioactive tritium. These functions are central to the operation of a tokamak and require a very robust design for all possible normal and off-normal conditions of the reactor. The blanket absorbs energy from fusion neutrons and incorporates different schemes for breeding tritium and removing heat from the reactor. The radiation shields (which can be considered as a part or an extension of the blanket) and vacuum vessel protect the magnets, external equipment, and personnel in the reactor building from the radiation produced from the interaction of fusion neutrons with reactor chamber wall materials. Access to the plasma volume is provided through the maintenance or access ports. These ports are employed for the replacement of wall blanket and divertor modules and insertion of instrumentation and neutral particle injectors. The heat absorbed within the blanket and divertor is removed by suitable coolants and transferred to one or more secondary loop coolants that employ the Rankine (steam) or Brayton (gas) cycle systems configurations to produce electricity or supply heat for process industries.

In the inertial confinement fusion (ICF), energy from lasers or particle beams is used for compressing the DT fuel by a factor of 1000–10,000 in order to achieve the necessary conditions for fusion. In the direct drive ICF, the energy is deposited directly onto a small (about 4 mm) target containing the DT fuel which is encapsulated within a protective gold cover maintained at about 18 K. In the indirect drive ICF, however, the lasers or particle beams deposit their energies onto a small cylindrical cavity (hohlaum) which contains the target. The high-Z materials of the hohlaum emit X-rays which irradiate the target and cause it to compress by implosion to fusion ignition conditions lasting less than a microsecond. The fuel containing target pellets can enter into the reaction chamber by gravity or by being injected with high velocities, and the energy from fusion is absorbed in the surrounding wall of the chamber. Following each pulse of 0.1–10 Hz, the reaction chamber must be purged from fusion products, fuel reliably introduced into the chamber, lasers or particle beams powered with more than 100 MJ of energy, and the energy from radiation, neutrons, and ions removed from the chamber of about 15–20 m in diameter. Most of the temperature transients occur within 100 μm of the chamber wall surface. The regions beyond 0.1–1 mm are subject to quasi steady-state conditions and thus allow the use of chamber wall designs being developed for the magnetic confinement plasma reactor systems (Morley et al., 2006). The United States is pursuing the laser ICF strategy at the National Ignition Facility through the High Average Power Laser (HAPL) program (National Ignition Facility). The particle beams ICF strategy is being pursued at the Sandia National Laboratory through the Z-pinch Power Plant (ZP3) program (Olson et al., 2005). Here, the Z-pinch accelerator is used to compress the DT fuel targets and the energy released is absorbed by a thick curtain of flowing molten salt that serves both as the coolant and the tritium breeder. This power plant is envisaged to operate in a repetitive mode with about one cycle every 10 s and in a 10 torr background argon environment. The ICF technology is also being developed in other countries.

2.3. ITER and fusion power demonstration reactors

The International Thermonuclear Experimental Reactor (ITER) is the next generation tokamak whose technical objectives are to demonstrate the reliability of plasma confinement, net fusion energy production, compatibility of materials, efficiency of fusion-to-thermal energy conversion, tritium breeding, nuclear safety, maintainability, and reliability of reactor components (ITER, 2002). ITER is currently being built in Cadarache, France, by China, EU, India, Japan, Russian Federation, South Korea, and the United States (Fig. 3), and in the inductive mode of operation was designed to achieve a power gain of $Q > 10$, fusion power of 500 MW, first wall heat and neutron fluxes in excess of 0.5 MW/m^2, neutron fluence in excess of 0.3 MWy/m^2, plasma temperature of about 150 million K, and plasma burn times of 300–500 s (ITER, 2001, 2002; Smith and Ward, 2007; Shimada et al., 2007). Some of the released fusion energy stored as the kinetic energy of alpha particles will be used to maintain the required plasma conditions. A small fraction of the alpha energy will, however, leak out from the plasma volume across the closed magnetic field surfaces and be deposited on the plasma facing first wall of the reactor, while the remaining portion will be diverted to the divertor. In off-normal conditions, however, large portions of the energy contained within the plasma volume can be rapidly deposited onto both the first wall and divertor targets of the reactor. More than 97% of the energy carried by the neutrons and gamma rays (produced from the interactions of neutrons with blanket materials) will be deposited in the blanket and removed as heat from the reactor. Most of the remaining portion of this energy will be further absorbed within the vacuum vessel and within the toroidal magnetic field coils. These coils will be cooled by the liquid helium at 4.5 K and subjected to minimal neutron fluxes, because the neutrons significantly degrade the magnets' superconducting state. The energy contained in the radiation beyond the vacuum vessel is being judged to be acceptable for humans to conduct the necessary maintenance of the magnets and other reactor systems.

The ITER's blanket consists of 421 blanket modules. Each module is about 45 cm thick and constructed from two parts. The 15 cm thick front part of each module consists of 4–6 panels, with each panel made of 1 cm thick beryllium armor protection, 1 cm thick copper to diffuse the heat load, and of about 10 cm thick back steel structure. These first wall panels can be damaged by the off-normal plasma conditions and may thus require frequent repair or replacement. Beryllium has the advantage of being a good thermal conductor and a low-Z material that is non-reactive with hydrogenic isotopes escaping from the plasma volume, but it is toxic and easily sputters, which makes it unsuitable for tokamaks with duty factors or duty cycles that are larger than that of ITER. The ITER's divertor is also of modular construction and consists of 54 cassettes. Each cassette support the ion armor or target plates which are built from the high thermal conductivity tungsten and carbon-fibre composites (CFCs) where the peak heating locations exist. CFCs co-deposit with tritium and deteriorate substantially under neutron irradiation, which could make them unsuitable for first walls of reactors with large duty factors. Both carbon and tungsten are high-Z materials and are employed for their good thermal shock and fatigue resistances. The structures of both the blanket and the divertor are made from the austenitic stainless steel and are cooled by water. Together with the vacuum vessel, both the steel and water in the blanket serve the purpose of shielding the humans, magnets, and other reactor support systems.

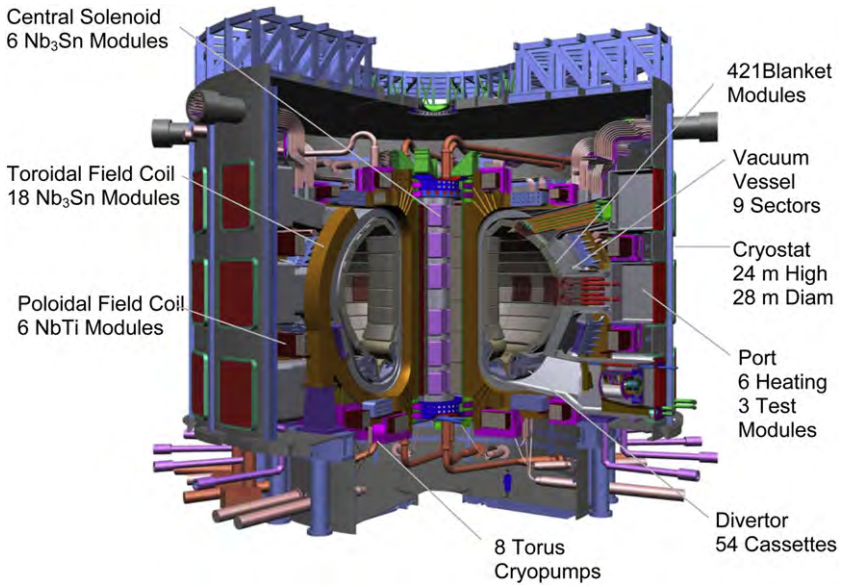

Fig. 3. The ITER tokamak cutaway (ITER, 2001, 2002). The structural material of the blanket and divertor is 316 SS. The first wall is built from Be and Cu-alloy heat sink panels. The divertor cassette armors employ W and CFCs. The vacuum vessel has a double-wall construction and is also built from 316 SS. The magnets are superconducting and operating at 4.5 K. Minor radius of the torus is 2 m, major radius is 6.2 m, and the toroidal magnetic field and current on the axis are 5.3 T and 15 MA, respectively. The plasma volume is 837 m^3 and the blanket and divertor are cooled with water at about 150 °C. Courtesy of ITER organization.

The tritium fuel will not be produced in ITER and will be supplied from external sources. Only about 1% of the tritium contained within the plasma will be 'burnt' and most will be recycled, which will require precise accounting to prevent its release into the environment. About one tenth of the fusion energy produced will be employed to power the magnets, neutral particle injectors, and other auxiliary systems. ITER will also aim at a steady-state operation of about 3000 s with a Q of at least 5, with the non-inductive current being produced from pressure gradients. ITER thus aims to demonstrate the scientific and technological feasibility of fusion power and spur the development of advanced reactor materials and wall blanket and divertor structures (with integrated cooling and tritium breeding systems) for the following design phase involving demonstration and commercial fusion power plants. The components of this reactor are currently being fabricated by the ITER partners and the reactor building phase will last for about 10 years and testing for another 20 years (ITER, 2002; Gasparotto, 2009). An International Fusion Materials Irradiation Facility (IFMIF) will also be built in parallel in Japan whose function is to test (employing two 5 MW deuteron accelerators striking lithium targets) the materials for use in ITER and in subsequent commercially oriented fusion energy producing reactors. Both the conventional and advanced high heat transport capacity and reduced-activation materials will be tested at this location (ITER, 2001).

It is anticipated that a generation of demonstration reactors (DEMOs) will be built following the operation of ITER and before the construction of commercial fusion reactor power plants. The DEMOs and subsequent reactors operating conditions will be, however, considerably different from those of ITER (Table 1), because of the necessity to produce competitive electricity cost and very robust power plants. The next step fusion energy producing plants will have to cope with sustained and intense plasma disruptions and disruptions related damage effects (material erosion, melting, vaporization) that can produce substantial levels of impurities into the plasma volume; large ion and neutron fluxes impinging on plasma facing components (PFCs); long pulse durations and large duty factors; routine operations with large amounts of tritium being recycled and the burnt tritium being replenished within the reactor; effective shields to protect the magnets and

Table 1
Parameters of the ITER and PPCS (ITER, 2002; EFDA, 2005; Maisonnier, 2008; Gasparotto, 2009; Mitteau et al., 2010) DEMO reactor models. The ARIES-AT (Najmabadi and The ARIES Team, 2006) is an advanced reactor design aimed at producing the electricity commercially. Li–Pb in this table is the short-hand notation for the compound of lead and lithium containing 17 mol% lithium and 83 mol% lead.

Parameter	ITER	Model A	Model B	Model C	Model *D*	ARIES
Electrical power (GWe)	–	1.55	1.33	1.45	1.53	1.00
Fusion power (GW)	0.5	5.00	3.6	3.41	2.53	1.7
Q	10	20	13.5	30	35	47
Major radius (m)	6.2	9.55	8.6	7.5	6.1	5.2
Minor radius (m)	2.0	3.18	2.8	2.5	2.03	1.3
Toroidal field on axis (T)	5.3	7.0	6.9	6.0	5.6	5.8
Plasma current (MA)	15	30.5	28.0	20.1	14.1	13
Ion temperature (keV)	8.5	22	20	16	12	18
Plasma density ($10^{20}m^{-3}$)	1.0	1.1	1.2	1.2	1.4	1.0
Neutron wall load (MW/m^2)	0.78	2.2	2.0	2.2	2.4	3.3
Heat load first wall (MW/m^2)	0.5	0.6	0.5	0.45	0.5	0.45
Divertor peak load (MW/m^2)	<10	15	10	10	5	5
Plant efficiency (%)	–	31	37	42	60	59
Blanket coolant	H_2O	H_2O	He	Li–Pb/He	Li–Pb	Li–Pb
T_{in}/T_{out} (°C/°C)	100/150	285/325	300/500	480/700 300/480	700/1100	700/1100
Divertor coolant	H_2O	H_2O	He	He	Li–Pb	Li–Pb
T_{in}/T_{out} (°C/°C)	100/150	140/167	540/720	540/720	600/990	700/1000
Breeder	–	Li–Pb	Li_4SiO_4	Li–Pb	Li–Pb	Li–Pb
Tritium breeding ratio	–	1.06	1.12	1.15	1.12	1.1
Blanket struct/ coolant liner	SS	SS	SS	SS/SiC	SS/SiC	SS/SiC
Divertor struct/ coolant liner	SS	SS	SS	SS	SS/SiC	SS/SiC
Divertor armor material	SS	W	W	W	W	W
Power conversion	–	Rankine	Rankine	Brayton	Brayton	Brayton

conduct remote maintenance of reactor components; stringent safety related procedures; etc. (Federici et al., 2001). The blankets and divertors of these reactors will have to employ advanced energy conversion concepts for removing the heat efficiently, and incorporate in the blankets self-sustaining tritium production cycles. High reliability of a fusion reactor requires a long service life (preferably 30–50 years) of its components and much simpler and more reliable fusion energy conversion schemes than are being anticipated today (see Section 3). This calls for the reactor's performance level that is several orders of magnitude higher than being achieved in current tokamaks. The DEMO goals essentially require the development of a safe, reliable, and economically competitive energy supply source that is sustainable for meeting the energy and environmental requirements of humanity far into the future. Several countries are pursuing the designs of DEMOs, but no final design will likely emerge until more effective reduced-activation and high duty factor resistant materials and simple, efficient, and reliable energy conversion schemes are developed and evaluated through the ITER and other projects.

The EU-commissioned Power Plant Conceptual Study (PPCS) (EFDA, 2005; Maisonnier, 2008) examined four model fusion reactor designs (A, B, C, D) as possible candidates for DEMOs. Models A and B are based on the extrapolation of ITER performance, whereas models C and D assume progressive improvements in plasma performance, use of advanced materials and coolants for neutron moderation and reactor cooling, and operation at high temperatures for improving the thermal efficiencies of power plants. All designs assume a power of 1.5 GWe delivered to the grid. The fusion power required to meet this demand decreases from 5 GW for Model A to 2.5 GW for Model D, because of the progressive thermal efficiency improvement of the plants. An EU DEMO would become operational 15–20 years after the ITER becomes fully operational by 2030 (Smith and Ward, 2007; Maisonnier, 2008). Some parameters of ITER and DEMO reactors are summarized in Table 1.

Model A DEMO employs water to cool the blanket and divertor and liquid Li–Pb (17 mol% Li and 83 mol% Pb) for breeding tritium. The state of water in this design at 15 MPa and 300 °C is similar to the pressurized water (fission) reactor (PWR) design conditions. Model B employs helium at 8 MPa and temperature of 300–700 °C for blanket and divertor cooling, and alternate layers of solid pebbles of Li_4SiO_4 and Be for breeding tritium and neutron multiplication, respectively. Model C employs a dual coolant configuration for cooling the blanket, where He is used to cool the blanket structure and Li–Pb for removing neutron-generated heat from the breeding zone of the blanket. Li–Pb is circulated through the silicon carbide (SiC)-lined tubes of the blanket to minimize the MHD effects and for breeding tritium. The divertors of models B and C are helium-cooled. Model D employs Li–Pb for cooling both the blanket and the divertor and for breeding tritium in the former. The coolant channels are lined with the SiC composite to allow operating temperatures above 1000 °C.

ARIES-AT (and other ARIES designs) is an advanced "commercial" 1000 MWe fusion power plant design developed in the United States (Najmabadi and The ARIES Team, 2006). This reactor employs the liquid metal Li–Pb at about 1000 °C for cooling the reactor blanket and divertor, and for tritium breeding in the former. The liquid metal heats a high pressure helium from 500 to 700 °C for use in the Brayton cycle to produce electricity or hydrogen. The channels through which Li–Pb flows are made of SiC liners, which act as insulators between the liquid metal coolant and the metallic structure of the blanket. The divertor is also cooled by Li–Pb. This permits a simpler cooling circuit design than the designs that employ separate cooling configurations for the blanket and divertor. Other ITER partners are also pursuing their own DEMO design strategies.

3. Materials and heat removal from fusion reactors

3.1. Fusion energy fluxes

A self-sustaining fusion reaction must produce more energy than is used to maintain the reaction and a figure of merit used to measure this performance is Q: The ratio of fusion energy released to the energy required to maintain an ignited plasma state. Q must be greater than one, but practically 10 or more is required for commercial reactors (ITER, 2002). About 20% of fusion energy (or 25% of neutron energy) is carried by the ions and in steady-state is absorbed through the divertor's surfaces. The remaining 80% of energy is carried by the neutrons and is absorbed within the blanket of the reactor. But because all existing tokamaks are subject to occasional rapid plasma termination events or 'disruptions', the plasma ions will in such situations deposit their energies on both the plasma facing first wall and divertor target surfaces and cause the atoms from these components to be ejected into the plasma. This physical sputtering, together with the chemical erosion, can produce significant erosion of PFCs and if not properly controlled can introduce significant amounts of cold ions and neutral atoms or impurities into the plasma volume and cause a loss of plasma confinement. The loss of confinement will, in turn, produce a rapid deposition of plasma thermal energy onto the PFCs, evaporation of material from PFCs, and additional transfer of impurities into the plasma volume. The control of these impurities in ITER and other tokamak reactor designs is achieved by employing open magnetic field lines residing on the outer edge of the plasma volume. The outermost closed magnetic field surface or separatrix of this volume defines the "X-point" or a zero of the poloidal magnetic field, below which resides the volume of the divertor. On and inside of this surface the magnetic field surfaces are closed and serve the purpose of confining the plasma, whereas on the outside of the separatrix the magnetic field lines penetrate the divertor's surfaces. The separatrix separates the inner edge region of the plasma and impurities and the outer scrape-off-layer (SOL) region of plasma and impurities, such that the magnetic field lines from the SOL guide the charged particles from both the edge plasma crossing the separatrix and from the SOL into the divertor where they deposit most of their energies before being pumped out of the machine and further processed to recover the large quantities of unburnt deuterium and tritium. The interaction of plasma with PFCs is most intense in the vicinity of the 'strike point', where the separatrix intersects the divertor's vertical target plates (see Fig. 10 for ITER's divertor). In the steady-state, the sputtering and ablation from ions and atoms are, therefore, much more severe on the target surfaces of the divertor than on the plasma facing first wall, but during a loss of plasma confinement the latter can also experience very high rates of particle fluxes. Because these fluxes can produce significant damage to the blanket and divertor armors, these components must be properly protected to avoid frequent replacements and reactor down times.

The main functions of the divertor are, therefore, the removal of the helium reaction product and impurities and the protection of plasma in the plasma volume from the impurities originating from plasma–wall interactions. The blanket with integrated shields, on the other hand, has the threefold purpose of breeding tritium, converting the energy from neutrons to high grade heat, and shielding the superconducting magnets from neutron energy deposition and radiation. Both the first wall and the divertor's target surfaces must be equipped with suitable armor materials for controlling erosion and tritium deposition and retention.

It is anticipated that the plasma facing first walls of future reactors will be subjected to heat fluxes up to 1 MW/m^2 and neutron fluxes up to 5 MW/m^2, whereas the divertor surfaces will

be exposed to very high erosion rates and heat fluxes up to 15 MW/m^2 (Table 1). The plasma confined within the torus is subjected to different types of disruptions that cause the ions to deposit their energies on the PFCs. These transient events of milliseconds (1–10 ms) durations can produce wall heat fluxes (1–100 GW/m^2) that are several orders of magnitude higher than the steady-state fluxes, causing ablation, melting, and vaporization of surface materials, producing cracks and tritium-induced contamination of materials, affecting plasma performance from the introduction of impurities into the plasma volume, etc. (Federici et al., 2001, 2002; Linke, 2006; Blanchard and Raffray, 2007; Ueda, 2008; Roth et al., 2009). The most critical plasma–wall interaction issues are the lifetime of PFCs, dust production from eroded PFCs, and tritium inventory in the vacuum vessel. These affect the tokamak operation in several ways. Erosion by the plasma determines the lifetime of PFCs, deposition of materials onto PFCs alters their surface composition and can lead to the accumulation of large in-vessel tritium inventories, and the retention and recycling of hydrogen from PFCs affect the reactor fuelling and thus plasma quality. These considerations determine, therefore, the choice of PFCs materials, such as beryllium, tungsten, carbon, CFCs, SiC, silicon carbide with silicon carbide fibre reinforced (SiC/SiC$_f$) composites, etc.

The neutrons damage the blanket materials through the atomic displacements and transmutations to near-neighbors in the periodic table. These displacements produce interstitial atoms and lattice vacancies that, under a certain threshold number of displacements per atom (dpa), cause volumetric swelling and loss of strength of the structural materials. Nuclear transmutations caused by (n,α) and (n,p) reactions produce H and He gases which cause microcracks that eventually lead to fracture. Such reactions cause the change of material composition and produce gamma rays and afterheat, leading to the reduced life of materials and the necessity of shielding the reactor from radiation. The first 10–15 cm of the chamber wall is a critical part of the fusion reactor, because the materials in this region lose their mechanical properties presumably after the neutron fluence of about 15 MWy/m^2.

In ICF reactors, additional complications arise from X-rays produced from the interaction of laser light and particles of ion beams with the fuel and hohlaum, background gas, and dry or wet first wall materials of the fusion chamber (IAEA, 1995). These issues are at the present poorly constrained and require additional studies. The envisaged power densities in tokamaks ($<$1 MW/m^3) are two orders of magnitude lower and in inertial confinement fusion reactors ($<$100 MW/m^3) are comparable to the current nuclear fission reactors (Abdou, 2007a). The damage that can be produced to the fusion chamber wall materials of both magnetic and inertial confinement fusion reactors by high energy neutrons, ions, impurities from plasma–wall interactions, and radiation can be severe and special materials are thus required to accommodate the mechanical, thermal, and nuclear loads (Ueda, 2008). In contrast to fission reactors, the fusion reactor are, however, subcritical and produce only a low level radioactive waste, which is easier to manage (Harms et al., 2000).

3.2. Materials compatibilities

To accommodate high fluxes of ions and neutrons the components of the fusion reactor chamber will have to be constructed from low neutron activation, low tritium retention, good thermal shock and thermal fatigue resistance over a wide temperature range, coolant corrosion tolerant, and high strength materials. The damage to PFCs and structural materials of the blanket can be reduced and heat transfer augmented by a liquid metal flowing along the inner surface of the chamber and with a liquid metal flowing within a porous metal or ceramic structure bonded to the blanket, but this concept also has problems (see below). The blanket requires a neutron multiplier (Be, Pb), a tritium breeder (liquids: Li, Li–Pb, Li–Sn, flibe, flinabe; solids: Li_2O, Li_4SiO_4, Li_2TiO_3, Li_2ZrO_3), one or more coolants (gases: He, CO_2; liquids: H_2O, Li, Li–Pb, Li–Sn, flibe, flinabe), and reduced-activation structural materials (such as ferritic/martensitic steels, vanadium- and niobium-base alloys, and SiC/SiC$_f$ composites) for meeting its functional requirements. The thickness of the blanket and shields must be sufficient to transform most ($>$95%) of the incident fusion energy into heat and shield the sensitive superconducting magnets from neutrons, because the neutrons degrade the magnets' superconducting state. The divertor can also employ similar structural materials and similar coolants as the blanket, but without the necessity to breed tritium. But because the divertor's target surfaces are exposed to the intense and sustained fluxes of ions and impurities they require special armors of refractory metals and ceramics to minimize the wall erosion and tritium retention.

The 14 MeV neutron irradiation giving rise to 1 dpa corresponds to the fluence of about 0.1 MWy/m^2 in steels. This reduces the thermal conductivity of material by some 80% and its life span to less than one year. Producing materials for DEMO reactors requiring 150 dpa (neutron fluence of 15 MWy/m^2) and higher at operating temperatures between 550 °C and 1100 °C presents, therefore, a great challenge (Zinkle, 2005a). High energy neutrons produce atomic displacements in materials, causing diffusion and concentration of vacancies and interstitials and transmutations to near-neighbors. Atomic displacement cascades induce the formation of point defects and segregation of alloying elements. Depending on the mechanical and thermal loadings, these material defects can produce embrittlement, plastic deformation, work hardening, short operating life span, and failures. When large quantities of H and He are produced through the transmutation reactions between the neutrons and materials they cause material phase instabilities, creep, volumetric swelling, and cracking. High He concentrations can produce material embrittlement at both high and low temperatures. These and the additional effects caused by cyclic thermal loading produce material fatigue, loss of ductility and strength, and changes of other mechanical, electrical, thermal, and chemical properties that render the material less resistant to the mechanical, thermal, electromagnetic, and nuclear loads (Zinkle, 2005a; Baluc et al., 2007; Suri et al., 2010).

The fusion chamber wall structural materials are, therefore, fundamental for maintaining the integrity of the reactor under the thermal and mechanical cycling, neutron irradiation, and off-normal reactor conditions. They must sustain high temperatures for maximizing the power plant efficiency and possess low neutron activation properties. Body-centered cubic (bcc) and face-centered cubic (fcc) metals are generally preferred for structural materials, with fcc metals offering higher strength and lower ductility than bcc metals and thus lower work hardening capability. The ductile-to-brittle transition temperature (DBTT) separates the low temperature brittle fracture regime from the high temperature recrystallization (RCT) regime and it is necessary to ensure that the exposure temperature is maintained above the metal's DBTT and below RCT temperature window whenever a stress is applied. The elements C, Cr, Fe, Mn, Mo, and Ni are vital (and Al, B, Cu, Nb, Si, Ta, Ti, V, and W are useful) for building high strength steels, but only C, Cr, Fe, Si, Ta, V, and W are safe enough for use in fusion reactors. Low-activation elements are C, Cr, Fe, Si, Ti, V, and W and are produced as reduced-activation ferritic/martensitic (RAFM) steels (containing Cr, Ta, V, and W), tungsten- and vanadium-base alloys (containing Ta and Hf, and Cr and Ti, respectively), and SiC/SiC$_f$ ceramic composites. RAFMs (such as EUROFER97and F82H) can be used below 550 °C, whereas tungsten- and vanadium-base alloys (typified by Ta–8W–2Hf and V–4Cr–4Ti) can be employed below

1000 and 800 °C, respectively. The oxide-dispersion-strengthened (ODS) ferritic steels contain nano-size Ti-, Y- and O-rich nano-clusters that provide significant strength and creep resistance to 700 °C and more and can thus significantly improve the operating temperatures of steels (Raffray et al., 2010). This is because a high density of small Y_2O_3 or TiO_2 particles dispersed in a ferritic matrix distribute He into small bubbles that cause less material swelling (Klimiankou et al., 2003; Zinkle, 2005a). But (because of H and He accumulation and significant radioactivity of all refractories, except V-alloys) even these special materials require additional improvements before they can be employed in commercial fusion reactors.

The operating temperature windows of the materials are normally specified by the allowed radiation damage and thermal stresses and some of these windows for the materials of current interest to fusion technology (for neutron irradiation levels of 10–50 dpa) are summarized in Fig. 4. The lower temperature limits are generally determined by the radiation embrittlement and the upper temperature limits by the thermal creep, swelling from H and He implantations, and coolant compatibility/corrosion issues (Zinkle and Ghoniem, 2000). An increasing neutron exposure of materials increases DBTT limits at low temperatures and decreases the upper operating temperature limits. The irradiation creep and transmutation produce an especially dramatic decrease of thermal conductivity (and thus the operating temperature window) of SiC/SiC_f composites above about 10 MWy/m^2. Table 2 summarizes the neutronic characteristics (neutron displacement, H and He transmutation, radiation dose) of some potential first wall and blanket structural materials for the neutron fluence of 15 MWy/m^2. The materials are listed in the order of their increasing capability to tolerate neutron displacements, which does not necessarily correspond to their increasing abilities to tolerate H and He transmutations and radiation doses.

The RAFM steels (and in particular ODS steels) and vanadium-base alloys are currently being considered as the primary candidate structural materials for future fusion reactors. They are resistant to helium embrittlement at high temperatures and suitable for a variety of coolant and tritium breeding options and in particular for self-cooled lithium breeding blankets. The ferritic/martensitic steels are chemically compatible with He/Li–Pb, H_2O/Li–Pb, He/Li ceramic, and flibe/flinabe coolants/breeders. Vanadium alloys can be used with Li/Li coolants/breeders, and, in general, the refractory alloys are compatible with the liquid metals and salts of interest for fusion applications, with the impurities in the coolants being of major concern for corrosion. The chemical compatibility data of Li–Pb and Li–Sn mixtures with other potential structural materials appear to be lacking, but the promising candidates for Li–Sn cooled systems are V alloys and SiC/SiC_f composites (Zinkle and Ghoniem, 2000). The SiC/SiC_f composites can also be employed with He/Li–Pb, He/Li ceramic, and flibe/flinabe coolants/breeders (Abdou, 2007a,b), and because they can sustain operating temperatures below about 1050 °C (Zinkle, 2005b) they are also being considered as the important structural materials for some components of fusion reactors. There are, however, significant safety and waste disposal issues associated with the use of some of these materials for fusion reactor blankets (Table 2).

The materials suitable for PFCs are the refractory metals Cr, Ti, V, and W and their alloys with Hf, Nb, Ta, and Zr. They all have melting points above 1500 °C and are highly resistant to creep at high temperatures. Tungsten has the highest melting point temperature

Table 2
Approximate neutronic response of some first wall and blanket structural materials for applications in the next generation fusion reactors. The data correspond to the neutron fluence of 15 MWy/m^2. The dose and decay rates correspond to 3 years at 5 MW/m^2. Adapted from Stacey (2010).

Alloy	Damage rate (dpa)	H and He transmut. (appm)	Dose rate (Sv/h)	Decay heat (W/kg)
Copper	210	10,000	2000	1
Austenitic steel	170	11,000	4000	3
Ferritic steel	170	9000	1000	1
Vanadium alloy	170	5000	0.3	0.005
SiC/SiC_f composites	135	33,000	0.0001	0.00003
Niobium alloy	95	2500	4000	4
Molybdenum alloy	95	6000	500	0.3
Tantalum alloy	50	200	1,000,000	1000
Tungsten alloy	45	200	1000	10

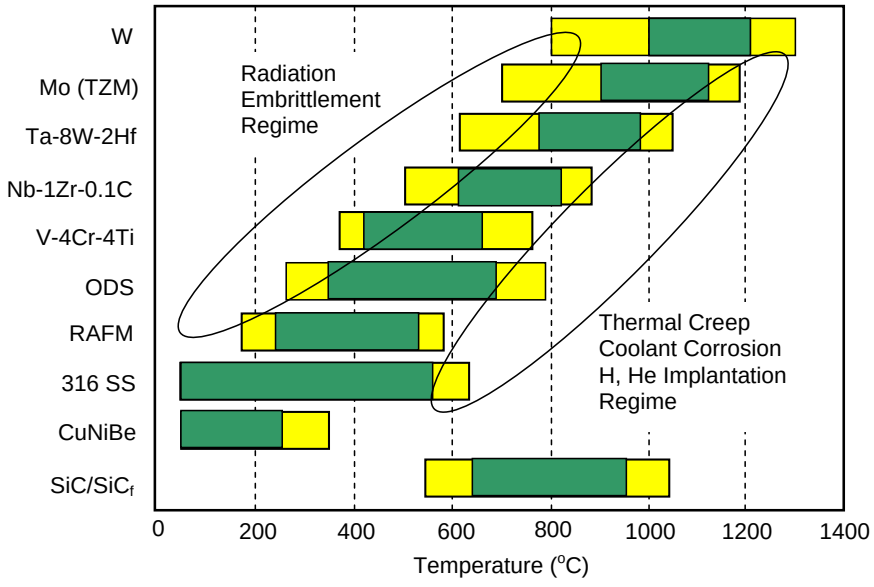

Fig. 4. Operating temperature windows of some candidate fusion reactor materials for the neutron irradiation giving rise to 10–50 dpa. The radiation embrittlement and thermal creep regimes delineate the minimum and maximum allowable operating temperature limits of these materials. Green (darker) areas indicate safe and yellow (lighter) areas marginal operating ranges. Adapted from Zinkle and Ghoniem (2000). [For interpretation of color in this figure legend, the reader is referred to web version of the article.]

(3422 °C) and low physical sputtering yield, no chemical sputtering in hydrogen plasma, does not co-deposit with hydrogen isotopes, possesses high thermal and shock resistant capacities, and is the preferred choice for the first wall and divertor target surfaces. Its shortcomings are that it loses ductility with temperature cycling from below and above DBTT and under neutron irradiation it suffers from H and He bubble formations that cause material swelling. Tungsten will melt under the anticipated thermal quench disruption loads and it will form the radioactive and highly volatile WO_3, but this could be taken care of by employing instead a W–Si compound which builds a protective layer of SiO_2 film at the interface when the metal comes in contact with oxygen compounds (Bolt and Roth, 2011). Tungsten's poor temperature window can be increased (600–1300 °C) by the addition of 1 mol% of La_2O_3 (WL10 alloy) (Norajitra et al., 2005).

Carbon does not melt but sublimes at high temperatures (>2200 °C). It has a good power handling and thermal shock resistance and preserves its shape under extreme temperature excursions, but its physical and mechanical properties degrade significantly under the neutron irradiation. Fibre reinforcement improves, however, the strength of fine grained graphite and is considered as the material of choice in ITER for the strike zone of the separatrix in the divertor (Norajitra et al., 2005). The SiC/SiC_f composites have high thermal conductivities (about 500 W/mK) and very low dose rates (about 0.0001 Sv/h). Their high H and He generation rates (about 33,000 appm for neutron fluence of 15 MWy/m^2) raise, however, a major feasibility concern of being employed in neutron-intensive environments (Stacey, 2010).

Liquid metals lithium, gallium, tin, and their compounds flowing along the plasma facing metal wall of the reaction chamber can rapidly remove large heat loads (50 MW/m^2), but their high evaporation (especially Li) at high temperatures, high corrosion, adverse MHD effects, and safety considerations degrade their practicality, unless special designs can be developed to mitigate these drawbacks. He bubble formation (from alpha ions) in liquid metals is not well understood and could produce liquid surface erosion and splashing and damage to the metal surface along which the metal is flowing. Plasma blobs injected into the plasma edge and crossing the SOL layer and reaching the liquid metal surface may disrupt the efficiency of the liquid metal cooling process. The material surface heat absorption can be increased, and some of the above disruptive processes mitigated, with the first walls made of capillary porous systems with Li flowing within a Mo or SS mesh, whereas the material surface erosion can be reduced with B infiltrated into the first wall made of a W mesh (Noda, 1999; Evtikhin et al., 2000). These promising designs are currently poorly constrained and may not turn out to be very practical for use in the fusion energy technology.

The choice of functional materials for neutron multiplication and tritium breeding is limited and the available choices are Be, Pb, and its compounds for the former, and Li, Li–Pb, Li–Sn, and Li-base ceramic materials (Li_2O, Li_4SiO_4, etc.) for the latter. The concern here is the copious amounts of H and He isotopes being produced in these substances and the penalty of magnetic field on liquid metal pumping when the liquid metals flow perpendicular to this field.

The ITER's first wall panels and blanket modules are being built from beryllium, Cu–Cr–Zr alloy, and austenitic stainless steel (316 SS) because they have the greatest technological maturity and are compatible with water for heat removal and able to resist modest neutron fluences. The armor tiles of the divertor are built from tungsten and carbon-fibre composites to mitigate the effects of high ion fluxes, whereas its substructure is built from the austenitic stainless steel (Barabash and The ITER International Team, 2007). Its coolant tubes are built from Cu–Cr–Zr alloy and include swirl tube inserts to increase the heat transfer carrying capacity. The ITER's divertor was designed to accommodate 10 MW/m^2 fluxes in steady-state and up to 20 MW/m^2 heat fluxes for less than 10 s (Raffray et al., 2010). Beryllium has a low risk of plasma contamination, but its physical sputtering yield is high, is toxic, co-deposits with tritium, and the neutron irradiation causes brittleness. The eroded carbon also co-deposits with tritium and as an impurity entering the plasma volume dilutes the fuel and reduces the plasma quality. The Be and C shortcomings may be tolerable in ITER, but will not be acceptable in DEMOs and next step commercial fusion reactors.

The energy conversion systems of DEMOs and subsequent commercial reactors will have to be built from the materials that can withstand the corrosion from high temperature coolants and suffer minimal neutron damage, while accommodating suitable tritium breeding schemes and support the mechanical and electromagnetic loads. The plasma facing first wall, the blanket, and the divertor with its armor, will have to operate with high temperature (up to 1100 °C) coolants (He, liquid metals, molten salts) and under severe thermal and mechanical cycling caused by the temporary (several ms) plasma power disruptions up to 100 GW/m^2. The first wall and blanket must also be able to withstand high irradiation rates (neutron doses producing more than 150 dpa and transmuted helium and hydrogen concentrations of more than 1500 appm for metals and 10,000 appm for SiC). Carbon, beryllium, nickel, molybdenum, and niobium are not very suitable because they are highly activated. Tungsten also suffers radiation damage from helium ion implantation and blistering at the first wall, which results in the transfer of impurities into the plasma core. Boronization and siliconization can limit the production of these impurities and B impregnated into a W mesh structure of first wall can mitigate the damaging effects of plasma disruption heat fluxes (Wong, 2009). The operating temperatures (Fig. 4), and corresponding thermal conversion efficiencies (Fig. 5), progressively increase with RAFM steels, ODS steels, vanadium-base alloys, SiC/SiC_f composites, and tungsten. Considering the current rate of material advancements it is not unreasonable to expect that the tolerable radiation damage rates will exceed the current expectations.

Tritium is a radioactive isotope that decays by β emission with a half-life of 12.3 years. It can diffuse rapidly through most materials and coolants, and thus its containment is difficult at elevated temperatures. A considerable amount of tritium in the plasma

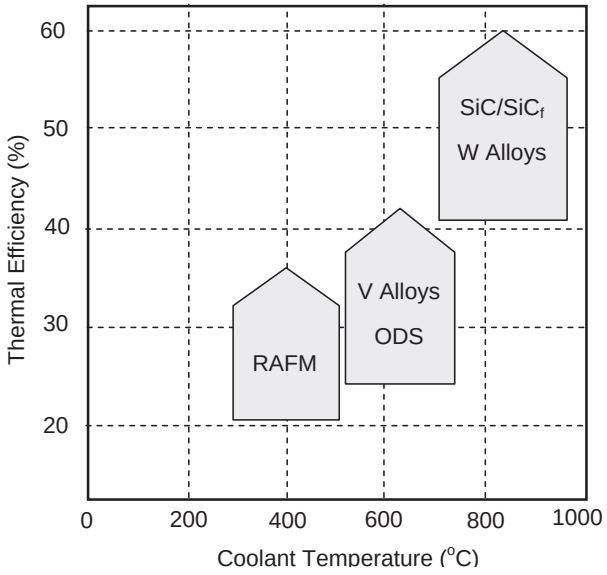

Fig. 5. Fusion reactor coolant temperatures and thermal conversion efficiency ranges achievable with candidate structural materials RAFM and ODS steels, V- and W-alloys, and SiC/SiC_f composites.

(envisaged to be 99% in ITER and as high as 70% in some ARIES reactor designs) will not burn and therefore will be exhausted through the divertor. Some tritium will also be co-deposited with the dust from plasma–wall interactions and will have to be recovered. The tritium fuel cycle must thus recover tritium from PFCs, breeding blankets, coolants, and exhausted materials from the divertor, store the fuel to maintain a sufficient inventory, and introduce the fuel reliably into the plasma chamber to power the reactor. The production and containment of tritium are, therefore, a major issue for fusion reactors and the aim of surface and wall conditioning techniques is to reduce the impurity fluxes from the walls and the control of hydrogen recycling (Philipps, 2004; Stacey, 2010). We will not discuss any further the many details of this tritium fuel cycle processing system, but simply note that this cycle must be considered seriously in the design of fusion energy conversion systems, because an energy penalty will have to be incurred and safety issues will have to be addressed to maintain a continuous supply of this crucial fuel. We will further discuss in Section 3.4 how tritium is envisaged to be produced within the solid and liquid breeding blankets of future fusion energy producing reactors.

The selection of PFCs materials for the armors and structural materials for the blankets and divertors of the next step fusion reactors is, therefore, a compromise from the requirements of plasma performance (minimization of impurities contaminating the plasma); lifetimes of components under thermal, mechanical and neutron loads; safety (minimization of tritium and radioactive dust inventories); shielding reactor components on the outside of the vacuum vessel; and high efficiency conversion of fusion energy to electricity with suitable coolants. As discussed in the following section, both liquids and gases can be employed to remove the heat from the blankets and divertors of fusion reactors.

3.3. Coolants for fusion reactors

Fusion reactor coolants will have to remove large wall heat fluxes from blankets and divertors (up to 1 MW/m^2 from the first wall and 10 MW/m^2 from divertor armors in steady-state and possibly up to 100 GW/m^2 under plasma disruption situations), remain compatible with the structural materials of the reactor's chamber wall, serve the functional purpose of maintaining efficient tritium breeding within the blanket, produce minimal pumping powers, possess high thermal capacities, operate at high temperatures for maximizing the power plant efficiency, and satisfy the operational safety and practicability limits. The water-cooled blanket and divertor of ITER will operate considerably below the requirements of DEMOs, and thus the ITER's heat removal is not an issue. But one of this reactor's very important objectives is to test (under plasma burn conditions) advanced blanket and divertor modules for use in DEMOs and most of the ITER partners are involved in producing such modules. The coolants being considered are liquid water, He gas, and lithium-based liquid metals and molten salts. Each of these coolants has positive characteristics and shortcomings, when judged in terms of material, functional, thermodynamic, and safety requirements. A high operating temperature of the coolant produces a high energy conversion efficiency (Fig. 5), which implies a lower fuel cost and less generation of waste per unit of energy produced. This also demands more advanced materials for PFCs, blankets, and divertors than are currently available.

Water has the critical temperature and pressure of 374 °C and 22.1 MPa, respectively, and should be used whenever possible because of its good heat transfer characteristics, practicality, tolerable pumping power requirements, and non reactivity with stainless steels, but it cannot be used effectively with the low-activation refractory materials which require elevated operating temperatures (above 700 °C for W) to avoid embrittlement. Vanadium- and niobium-base alloys may also produce substantial levels of corrosion in water, titanium alloys are not suitable because of hydrogen embrittlement, whereas the high-nickel-base alloys are acceptable, but then the radiation embrittlement probably precludes their use. It is also difficult to extract tritium from water when it leaks into the coolant system (Stacey, 2010). Water is very reactive with liquid metals and when used in conjunction with the tritium breeder lithium it poses significant safety concerns in the event of a blanket rupture. The pressurized water (fission reactors operate at about 15 MPa) is, therefore, used with low temperature Rankine cycles (DEMO designs A and B (Table 1)) and yields low power plant efficiencies (30–35%). Boiling water can remove larger heat transfer fluxes, but these are limited by the critical heat flux (CHF) above which the heat removal effectiveness diminishes and heat transfer surface temperature increases rapidly.

Helium gas is inert and transparent to neutrons and integrates well with ceramic (Li_2O, Li_4SiO_4, $LiAlO_2$) and liquid (Li, Li–Pb, Li–Sn) tritium breeders. At low pressures, He requires large pumping powers and manifolds for effective heat removal, but this can be remedied with heat transfer enhancement techniques, such as extended surfaces, swirl tape inserts, surface roughening, porous media heat exchange, particulate addition, etc. (Baxi and Wong, 1999; Ihli and Ilić, 2009). Heat removal with the He gas is effective at high pressures (10–20 MPa) (Sze and Hassanein, 1993) and at high temperatures (500–1000 °C) and can be used in Brayton cycles with low reactivity refractory metals and ceramics to obtain high thermal conversion efficiencies (50–60%). He also integrates well with stainless steels and titanium and high-nickel-base alloys (<650 °C). However, the trace impurities (H_2, H_2O, CO, CO_2, CH_4, N_2, O_2) in He can produce the corrosion-embrittlement of vanadium, niobium, and molybdenum alloys (Stacey, 2010). Helium satisfies the inherent practicality and safety requirements and can remove 5–10 MW/m^2 heat fluxes from the first wall and divertor targets. MHD pressure drop and associated turbulence suppression are not important issues with He-cooled blankets and divertors. The high temperature operation with He requires, however, that the tritium breeding is compatible with refractory metal alloys and SiC/SiC$_f$ composites (Wong et al., 1994). High pressure coolants have the disadvantage of requiring more massive structures for containment, which increases the cost of energy production.

Low Prandtl number liquid metals Li and Li–Pb and Li–Sn mixtures have excellent heat transfer and neutron absorption qualities and can be used for the dual purpose as coolants and tritium breeders. Because of their reactivity with oxygen they are difficult to handle, corrode structural materials, and can produce large MHD pressure drops and associated flow laminarization that reduce their heat transfer capacities. Austenitic stainless steels (such as 316 SS) corrode in lithium above 400–450 °C, ferritic steels are more corrosion resistant, and both high-nickel and titanium alloys are unsuitable because of high solubility of alloying elements in lithium. Vanadium and niobium alloys have good corrosion resistance to lithium up to 800 °C (Stacey, 2010).

Short flow passages arranged parallel to the magnetic field reduce MHD effects, but they still need to be coated with insulating materials which are inadequately explored at the present (Raffray et al., 2002). When arranged in clever heat pipe configurations, the evaporating Li at 1200 °C can transport axial power densities of 200 MW/m^2 (Dobran, 1987). Heat transfer in heat pipes is, however, subject to hydrodynamic, boiling heat transfer, and magnetic field limits that have not yet been adequately investigated for applications to fusion reactor environments.

Typical liquid metals considered for fusion reactor cooling are Li and Li–Pb (eutectic mixture of 17 mol% Li and 87 mol% Pb) because

of their tritium breeding potential and low melting and high boiling temperatures at low vapor pressures. Lithium has the melting temperature of 181 °C and its very low vapor pressure makes it suitable for near-vacuum operation of first wall and other structures within the vacuum vessel of the reactor. Li–Pb has the melting temperature of 234 °C and considerably larger density, heat capacity, and thermal and electrical conductivities than Li. This makes this liquid metal mixture a superior heat transfer fluid in the absence of magnetic fields and non-acceptable for use in high magnetic field environments. Li–Sn (eutectic mixture of 25 mol% Li and 75 mol% Sn) has the melting temperature of 330 °C and at near-vacuum pressures (10^{-4} torr) has exceptionally high (727 °C) evaporation temperature, but its tritium breeding potential is significantly lower than that of Li or Li–Pb. The liquid metals gallium and tin have even better rear-vacuum operating temperatures and pressures for use as liquid films flowing along the plasma facing metal walls of the reactor (Table 3) and their compatibilities with these components is further discussed in Section 3.5.5. MHD pressure drop, turbulence, and electrical conductivity of flow passages are very important issues with liquid metals. In magnetically confined plasma fusion reactors cooled by liquid metals, special precautions are thus necessary, such as: Elimination of high flow velocities and electrical conduction between the coolants and metal walls, avoidance of coolants flowing transversely to the magnetic field, and elimination of contacts with oxygen compounds (air and water).

Molten salts are high Prandtl number fluids which exhibit thin thermal boundary layers where the wall turbulence is the primary mechanism of heat transfer. Flows perpendicular to the magnetic field reduce this turbulence and heat transfer enhancements may be necessary to promote the heat transfer. MHD pressure drop and electrical insulation of flow passages are not very relevant issues, but the buoyancy effects may be if the flow velocities are low. There are various types of molten salts involving binary and ternary mixtures with a wide range of melting and boiling points (IAEA, 2009). Nitrate, sulphate, and carbonate salts contain oxygen and are thus unsuitable. Chloride salts are corrosive and become neutron activated, and are also unsuitable. The fluoride salts flibe ($LiF–BeF_2$) and flinabe ($LiF–NaF–BeF_2$) are chemically stable at high temperatures, and can be used for the dual purpose as reactor coolants and tritium breeders. Beryllium in fluorides serves as a neutron multiplier (n,2n) for tritium breeding. Flibe has the melting and boiling temperatures of 360 °C and 1430 °C, respectively, and vapor pressure of 10^{-5} Pa (at 380 °C). It is non-reactive in air and water, stable at high temperatures relevant to fusion reactor environments, and has a low MHD resistance compared to Li and Li-Pb. Its breeding capabilities are limited and must be incorporated with Be. Beryllium also stabilizes fluorine in the salt and makes it less aggressive with candidate structural materials. The low melting temperature of flinabe (308 °C) and its vapor pressure and heat transfer properties similar to flibe makes this coolant more suitable than flibe. The interaction of fluoride salts with reactor chamber materials is, however, of major concern. Fluoride constituents LiF, BeF_2, and NaF react with Cr, Fe, Mo, and Ni, and produce corrosion fluorides, but they do not react with SiC composites. Unfortunately, the transmutation of lithium in flibe and flinabe produces very corrosive tritium fluoride species (TF). TF behaves like hydrofluoric acid and can rapidly degrade the structural materials of the reactor (Farmer, 2008).

The choice of a coolant for fusion reactor depends, therefore, on the compromise between the fusion chamber wall materials, its function as only a coolant or both as a coolant and tritium breeder, thermodynamic requirements to produce a high thermal conversion efficiency, cost of the produced electricity or heat, and on the amount of nuclear waste per unit of energy being produced. These and other fusion reactor parameters determine a set of sustainability indicators for assessing the fusion energy as a viable (sustainable) energy source (Dobran, 2010, 2011).

3.4. Fusion reactor blankets

ITER provides an opening port in the chamber wall of the reactor (Fig. 3) for evaluating Test Blanket Modules (TBMs). These modules are intended to provide a design base for use in the following generation of DEMO reactors and several designs have been proposed for this purpose. These designs employ some of the materials, tritium breeders, and coolants identified above, and are based on the detailed mechanical, neutronic, and thermal analyses. Our purpose in this section is to provide a sampling of these and other designs, for the purpose of identifying the considered technologies and thus provide impetus for more effective design strategies needed to build the commercial fusion energy producing systems. TBMs can be conveniently grouped into the solid and liquid breeder concepts (Abdou, 2007b, 2010).

3.4.1. Solid breeder blankets

Solid breeder blankets are always separately cooled with either helium or water. Tritium is bred in a stationary lithium ceramic (Li_2O, Li_4SiO_4, Li_2TiO_3, Li_2ZrO_3) surrounded by or adjacent to a stationary neutron multiplier bed consisting of Be or Be–Ti (82 mol% Be and 12 mol% Ti). Li_2O has a superior thermal conductivity and tritium breeding potential, but a lower operating temperature window (400–800 °C) for breeding and is more reactive with water than other solid breeders. Be–Ti is less chemically reactive than Be and is a better choice. A low pressure helium (0.1 MPa) is used to purge tritium from the ceramic breeder and a high pressure (8 MPa) helium or water are employed to cool the first wall and blanket internals. These coolants are compatible with the currently available RAFM steels for use as the blanket structural materials and allow operating temperatures up to 550 °C.

Table 3
Properties of candidate liquid metals and molten salts for applications to fusion reactor liquid walls and capillary pore systems (Davison, 1968; Gierszewski et al., 1980; Zinkle, 1998; Sharafat and Ghoniem, 2000); Zaghloul et al., 2003; Williams et al., 2006; Fukuda et al., 2007; Samuel, May 2009). Li–Sn consists of 75 mol% Sn and 25 mol% Li; flibe consists of 48 mol% LiF and 52 mol% BeF_2; flinabe consists of 31 mol% LiF, 32 mol% NaF, and 37 mol% BeF_2; and Li–Sn consists of 25 mol% Li and 75 mol% Sn. The operating pressure of the reactor (between 10^{-7} and 10^{-4} torr (1.33×10^{-5} and 1.33×10^{-2} Pa) determines the operating upper temperature window of the coolant (Stacey, 2010).

Coolant	Li	Ga	Sn	Li–Sn	Flibe	Flinabe
Atomic number	3	31	50	–	–	–
Atomic weight	6.9	69.7	118.7	90.8	36.9	38.9
Melting point (°C)	181	29.8	232	330	360	308
Boiling point (°C)	1347	2200	2620		1430	1400
Liquid density (kg/m^3)	500	5900	7000	6000	2080	2000
Heat capacity (kJ/kg°C)	3.6	0.4	0.23	0.32	2.4	3.8
Thermal conductivity (W/mK)	85	41	67	43	1	0.9
Electrical resistivity (nΩm)	0.9	600	115	6000	10^7	10^7
Saturation temperature (°C) for pressure $10^{-7}/10^{-4}$ torr	277/402	620/830	780/980	441/727	382/532	415/600

A proper integration of coolants and breeders should account for the exponential decrease of neutron energy from the first wall, optimal breeder performance (grain size, porosity, microstructure, tritium breeding temperature window, chemical activity), effective heat removal, and materials compatibility. The breeding materials in solid breeders are normally arranged in pebble bed modules that are integral parts of TBMs. Solid breeders have the advantage of maintaining the tritium inventory and their corrosion effects localized, and since they are stationary they have no MHD pumping power penalties. Their shortcoming is poor power densities because of low thermal conductivity of breeder ceramics. Solid breeder blanket issues are associated with the mechanical and thermal cycling effects, poor definition of heat and mass transfer parameters, and (radioactive) tritium inventory control.

Helium Cooled Pebble Bed (HCPB) and Water Cooled Pebble Bed (WCPB) blankets have been proposed by China, EU, India, Japan, South Korea, and US. They are designed to fit within the ITER's TBM port for evaluation. The European design of HCPB includes both horizontal and vertical configurations (Boccaccini, 2001; Cismondi et al., 2009), with the most recent vertical design (Fig. 6) incorporating 16 ceramic breeder (Li_4SiO_4) cell units (left drawing in the figure) containing 0.2–0.6 mm pebbles. The cells are stacked in two toroidal and eight poloidal directions, with each cell employing beryllium (in the middle) for neutron multiplication. High pressure (8 MPa) He is first circulated radially and toroidally along the first wall of the blanket and then through the cooling passages encapsulating the breeder cells (right drawing in Fig. 6). A separate loop of low pressure (0.1 MPa) helium is used to purge tritium from the pebble bed cells and from the module. The maximum neutron wall loading and surface heat flux for this TBM are 0.78 MW/m^2 and 0.5 MW/m^2, respectively, and the He coolant inlet and outlet design temperatures are 300 °C and 500 °C, respectively. The upper operating temperature of the module (550 °C) is determined by the structural material RAFM steel EUROFER and the neutron damage allowed is about 50 dpa. China, India, South Korea, and US are proposing similar TBM designs, with the variations in coolant-breeder-neutron multiplier arrangements (Abdou et al., 2007; Ahn et al., 2008; Feng et al., 2008; Chaudhuri et al., 2010). The HCPB breeding blanket is the only concept that most of the ITER partners are interested in developing and will most likely be the first to be tested in this machine.

Japan's vertical TBM for testing in ITER employs water as the coolant, lithium titanate (Li_2TiO_3) for tritium breeding, and Be for neutron multiplication. Pebbles of tritium breeder and neutron multiplier are arranged in layers, and between the layers membrane panels with water cooling pipes are employed to remove the heat. Water at 15.5 MPa and 280 °C enters and at 325 °C exits the module, and removes the first wall heat load up to 0.5 MW/m^2. The first wall is made from the beryllium armor tiles and the RAFM steel is employed as the structural material of this TBM (Akiba et al., 2010). The Japanese DEMO design (Tobita et al., 2010) also involves water as the blanket coolant, but replaces lithium titanate with Li_4SiO_4 and Be with Be–Ti (12 mol% Be, 98 mol % Ti) as the tritium breeder and neutron multiplier, respectively. Be–Ti does not react with hot water in the event of coolant boundary malfunction and Li_4SiO_4 is superior for tritium breeding, thus allowing for a simpler blanket design. In the most recent design, both are mixed as pebbles in the blanket module through which circulates water at subcritical conditions in poloidally arranged tubes. This breeder-coolant arrangement is simple and can remove large neutron and heat loads (<5 MW/m^2), and was designed to take advantage of some of the light water (fission) reactor technology (heat exchangers, turbines) which operates with similar subcritical water conditions. The subcritical water cooling produces, however, a low thermal efficiency of the plant and reduces the tritium breeding ratio because of the large water inventory in the blanket. Some Japanese DEMO designs employ water at supercritical conditions (540 °C) and produce higher thermal efficiencies (40–45%) (Terai, 2001).

Solid breeder blankets offer good compatibility between the breeder, coolant, and structural materials, and thus lessen the problems related to safety, corrosion, and MHD effects. A large

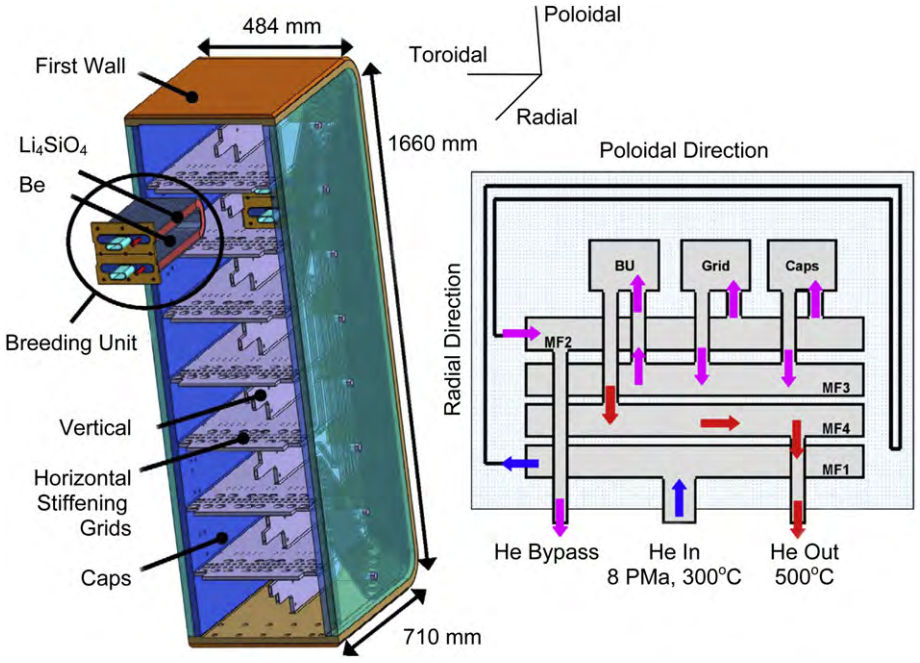

Fig. 6. European HCPB TBM (Cismondi et al., 2009). Sixteen breeding-neutron multiplying units are arranged in two toroidal and eight poloidal directions (left). The structure of the module is built from the RAFM steel EUROFER, designed to withstand the maximum operating temperature of 550 °C. High pressure He is used to cool the module (right) and low pressure He for purging tritium from breeding units (not shown). ©2009 Elsevier, reproduced with permission.

tritium inventory in the breeder causes safety concerns and requires the development of tritium permeation barriers. Their major drawbacks are the limits on power densities due to low thermal conductivities of breeder materials and on blanket lifetime caused by radiation damage and burn-up of breeder materials (Terai, 2001). Note, however, that neither of the above HCPB TBMs are suitable for building high efficiency DEMOs. Higher neutron and heat load densities can be tolerated and tritium breeding ratios can be produced with liquid breeder blanket designs which we consider next.

3.4.2. Liquid breeder blankets

Liquid breeders employ liquid metals Li and Li–Pb and molten salts flibe and flinabe as both tritium breeders and coolants of blankets in several configurations: (1) self-cooled configuration, where a liquid breeder circulates at high speed through the blanket and cools the blanket; (2) separately cooled configuration, where a coolant (usually He) is used to cool the blanket and a breeder liquid metal or flibe/flinabe is slowly circulated to extract tritium; and (3) dual coolant configuration where a coolant such as helium is used for removing heat from the first wall and blanket structure and a coolant-breeder is employed for both, producing tritium and extracting heat from the breeder zone. Liquid breeders have the potential for high power densities and for employing Pb in Li–Pb as the neutron multiplier. They offer long lifetimes of breeder materials due to the replenishment of Li on-line as it is being used up. Lithium can be used with the vanadium alloys, and Li–Pb, flibe and flinabe with the ferritic steels and refractory metals and SiC/SiC_f composites up to 1000 °C (Raffray et al., 1999a; Abdou, 2007a). Flowing liquid metal designs can be simple, but their MHD effects couple with heat and mass transfer differently in the inboard and outboard blanket modules and in electrically conducting and insulating flow passages. Due to the high intensity volumetric heat generation and low circulation velocity to maintain tolerable MHD pressure drops, liquid metal flows in these devices can experience problems with buoyancy, hot spots, and tritium accumulation and permeation. This may require insulated coating structures and clever designs of flow configurations (Mistrangelo and Bühler, 2009; Smolentsev et al., 2010; Zhang et al., 2010; Yang et al., 2010). Flibe and flinabe have lower chemical activities and MHD effects than liquid metals, but they also have lower heat transport capacities and tritium breeding ratios, which limit their power densities. Salts have issues with corrosion of some TBM materials and require Be for producing an acceptable tritium breeding ratio.

Several ITER partners are designing Helium Cooled Lead Lithium (HCLL) TBMs for testing in this reactor and eventual use in DEMOs (Poitevin et al., 2010). In these designs, helium is used for cooling of the first wall and blanket internals and Li–Pb for breeding tritium. Such a mixture of lead and lithium has a low melting temperature and flows through the breeding units of the blanket at low velocities for easy tritium recovery and avoidance of MHD penalties. The MHD pressure drop in a breeding unit is less of an issue as when these units are integrated into a blanket module which contains more than a dozen of such units. The European design of vertical HCLL TBM (Fig. 7) (Salavy et al., 2008) employs the RAFM steel EUROFER for the structural material of the module. Each module holds 16 breeder-neutron multiplier units and is similar to the HCPB design shown in Fig. 6. The breeding units and the plasma facing and sidewalls of the module are cooled by the high pressure helium at 8 MPa, where its inlet and outlet temperatures are 300 °C

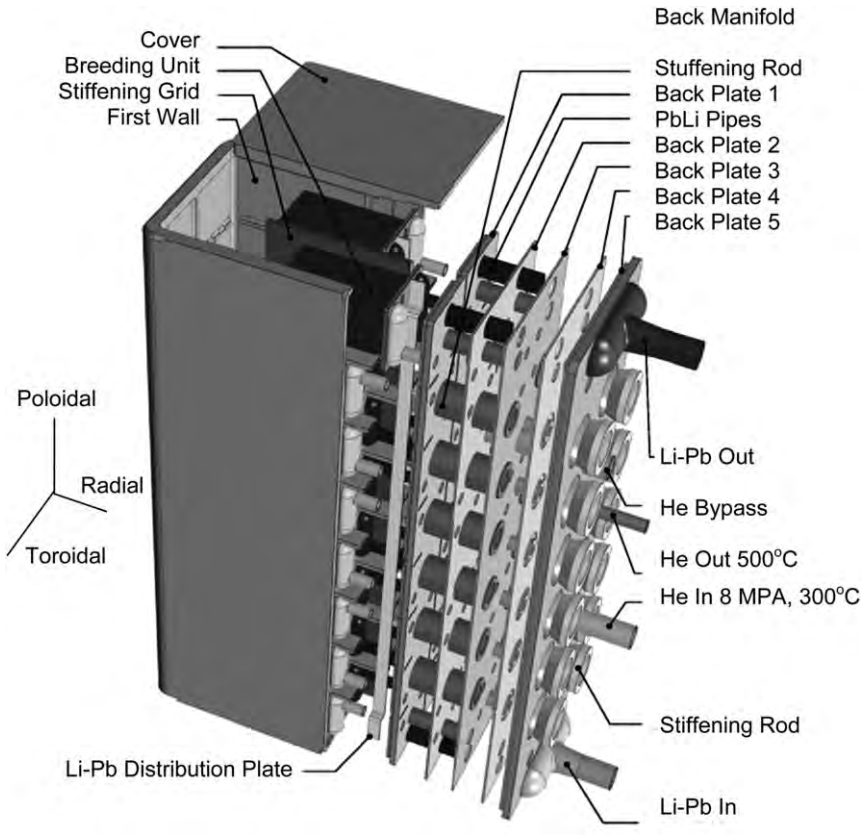

Fig. 7. European HCLL TBM (Salavy et al., 2008). Sixteen breeding-neutron multiplying units are arranged in two toroidal and eight poloidal directions. The overall module dimensions and the He flow arrangement are similar to the HCPB design as shown in Fig. 6. The structure of the module is built from the RAFM steel EUROFER. ©2008 Elsevier, reproduced with permission.

and 500 °C, respectively, and its internal flow arrangement is similar to that of Fig. 6 (right). The amount of Li–Pb circulating through the breeding units and the tritium being recovered from the module are managed by a tritium fuel cycle processing system.

In a self-cooled Dual Coolant Liquid Metal (DCLL) TBM, both a high pressure He and a low pressure Li–Pb coolant-breeder are used to cool the blanket. Helium is employed to remove the heat deposited in the blanket structure and Li–Pb is used for both, breeding tritium and removing the neutron-generated heat from the breeding zone. Because the liquid metal circulates with non-negligible velocities through the breeding units, it normally requires electrically insulated flow channels to reduce the liquid metal MHD pressure drop, unless the metallic flow passages are arranged predominantly parallel to the toroidal magnetic field or liquid metal flows with very low velocities. An additional advantage of such channels is that they are also good thermal insulators, which permits the liquid metals to work at higher temperatures than those of the surrounding metal structures. Another possibility is to use flibe or flinabe instead of liquid metals, but this could reduce the blanket's power density, cause laminarization of thermal boundary layers that reduces the heat transfer, and (like liquid metals) may produce corrosion problems. The flow laminarization can, however, be used to an advantage, because it allows the molten salt to operate at higher temperatures than the surrounding blanket structure whose operating temperature window can be lower.

Some American ARIES and European PPCS fusion power plant designs (Table 1) employ the DCLL technology. The American TBM shown in Fig. 8 (Abdou et al., 2007) incorporates ceramic flow channel inserts (FCIs) embedded into the RAFM steel structure of the module. FCIs (0.2 m wide, 0.2 m deep, 2.0 m high) are made of SiC/SiC_f composite and through them circulates a low velocity Li–Pb to produce tritium and remove the neutron energy deposited in the breeder region. The 5 mm thick flow channel inserts are embedded into the steel structure which together with the first wall is cooled by helium. High pressure (8 MPa) helium is heated from 350 to 410 °C and the liquid metal Li–Pb flowing counter-currently through the FCIs is heated from 360 to 470 °C. The maximum neutron and heat flux loadings on the 2 mm thick Be first wall of this module are 0.78 MW/m^2 and 0.5 MW/m^2, respectively. The flow channel inserts of this design provide a reduction of the MHD pressure drop by a factor of 100 over the uninsulated channels. The choice of using insulating channel inserts instead of coatings comes from the difficulty of maintaining the integrity of the latter in extreme fusion reactor environments.

Insulating flow channel inserts do not have to be used with the coolant-breeder molten salt flibe or flinabe. Molten salts do not produce intolerable MHD pressure drops, but may require turbulence promoters to increase the reactor power densities. These salts can also operate at high temperatures with SiC/SiC_f composites and thus produce high thermal conversion efficiencies. The Dual Coolant Molten Salt (DCMS) blanket module shown in Fig. 9 employs both helium and a molten salt (flibe or flinabe) to cool the first wall and blanket internals (Sawan and Youssef, 2006). The toroidally oriented He cooling channels remove heat from the 3 mm thick first wall. These are then followed by molten salt channels in front and back of the 5 cm thick Be pebble bed multiplier zone. Following these are the He-cooled poloidal channels forming the large channels for the molten salt to flow in the poloidal direction. Helium removes heat from the metal structure of the blanket and the molten salt breeds tritium and removes the neutron-generated heat from the module. Because of the flow laminarization in the molten salt, the temperature of this coolant-breeder is about 100 °C higher that that of the surrounding metal structure temperature, which allows for an increased thermal conversion efficiency of the blanket. This blanket module design forms a part of an advanced 2.1 GW fusion power reactor, which (with the He inlet/outlet temperatures of 300 °C/450 °C and molten salt inlet/outlet temperatures of 500 °C/700 °C) can produce the thermal conversion efficiency of 48%. When such a blanket and first wall are built from the reduced-activation ferritic steel and its first wall is exposed to neutron loads up to 3.72 MW/m^2, its expected lifetime is about 7 years, assuming the radiation damage limits of 200 dpa and 2500 appm. The breeding ratio produced by this design is 1.07.

The PPCS DEMO Model C (Table 1) also employs a dual coolant (He and Li–Pb) technology and the blanket module design for this reactor is similar to that as shown in Fig. 8, except for the dimensions of blanket modules (3 m toroidal, 2 m poloidal, 1 m radial) which are larger and fewer in number (176) in order to reduce the thermal stresses from plasma disruptions (Norajitra et al., 2003). In this design, He is used to cool the RAFM steel structure of the blanket and Li–Pb flowing in 5 mm thick SiC/SiC_f flow channel inserts to breed tritium and remove the neutron-generated heat

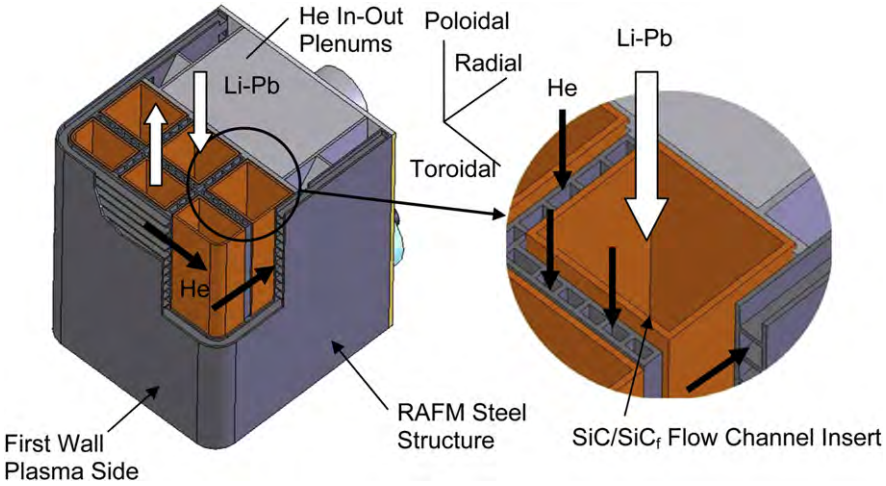

Fig. 8. American DCLL TBM (Abdou et al., 2007) employs SiC/SiC_f flow channel inserts which provide the thermal and electrical isolation between the high temperature liquid metal Li–Pb flowing through the channels and the lower temperature He employed to cool both the Be first wall and the ferritic structure of the module. The module is 484 mm wide, 1660 mm high, and 413 mm deep. The liquid metal Li–Pb produces tritium and removes the neutron-generated heat from the breeding zone. ©2007 UCLA, reproduced with permission.

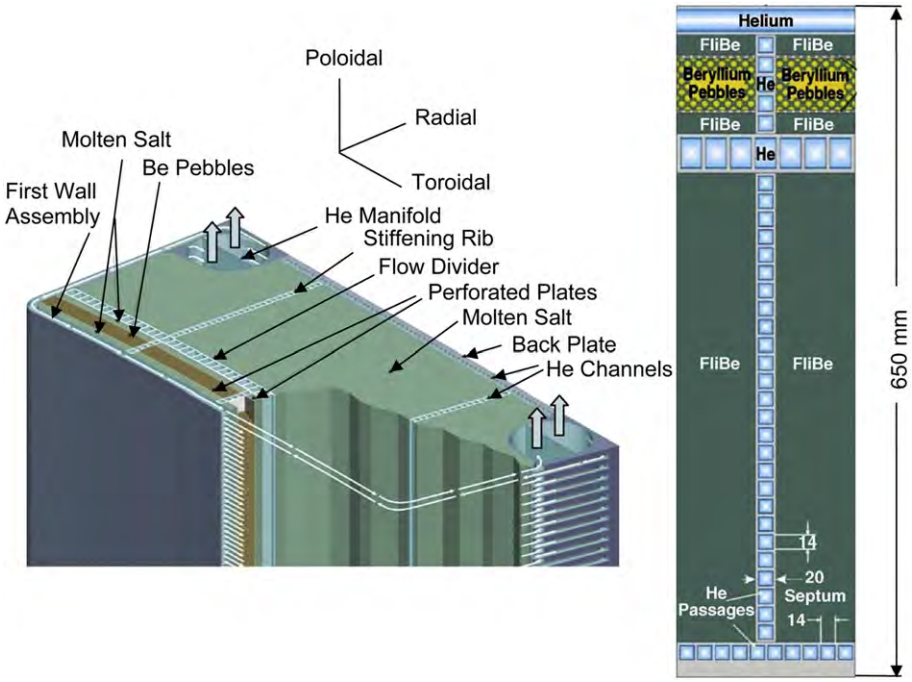

Fig. 9. American DCMS TBM (Sawan and Youssef, 2006) employs He to cool the first wall and the ferritic metal structure of the module, and the molten salts flibe or flinabe to breed tritium in the Be pebble beds and remove the neutron-generated heat from the blanket. The inlet and outlet temperatures of He are 300 °C and 450 °C, respectively, and the inlet and outlet temperatures of molten salt are 500 °C and 700 °C, respectively. ©2006 Elsevier, reproduced with permission.

from the breeding zone of the blanket. This allows for the Li–Pb inlet/outlet operating temperature of 470 °C/700 °C and for the He inlet/outlet temperatures of 300 °C/480 °C. To increase the operating temperature of the first wall (from the allowed 550 °C for the ferritic steel) to 650 °C, the fist wall is coated with a 3 mm thick layer of ODS steel. Helium flows trough the blanket at about 8MPa, and through the divertor at about 10 MPa where its temperature increases from 500 to 720 °C. The average neutron and heat wall loads for the blanket are 2.27 MW/m^2 and 0.6 MW/m^2, respectively, and the calculated breeding ratio is 1.15. With a secondary He loop operating at high pressures (15–18 MPa), it is possible to achieve with this blanket design the thermal conversion efficiency of 44%.

The blanket of the American ARIES-ST commercial fusion reactor is also a variation of the design shown in Fig. 8 and PPCS Model C design. Its ferritic steel structure was designed to withstand the first wall neutron and heat flux loads of 6 MW/m^2 and 0.6 MW/m^2, respectively, He inlet/outlet temperatures of 300 °C/525 °C, and Li–Pb inlet/outlet temperatures of 550 °C/700 °C. The peak heat flux load on the divertor surfaces is 6 MW/m^2. This 2.8 GW fusion power reactor was designed to produce the thermal efficiency of 45% (Tillack et al., 2003).

The current designs of tokamak fusion reactors are limited by the relatively low operating temperatures of energy conversion systems (blankets and divertors). The ferritic/martensitic steels are the preferred structural materials for the components of these systems and the SiC/SiC$_f$ composites are the choice materials for the coolant channels within the blankets when using liquid metals. Helium is employed to remove the heat from the beryllium- or ODS-coated first walls and keep the blanket structures below the RAFM operating temperature limit of about 550 °C. Both, the liquid metal Li–Pb and the molten salts flibe and flinabe are employed for breeding tritium, removing neutron-generated heat from the breeding zone, and for operating at higher temperatures than the He coolant, thanks to the liquid metal flowing through the blanket in (insulating) ceramic channels and the molten salts experiencing flow laminarization from the magnetic field. These design features produce fusion reactor thermal conversion efficiencies below about 45%. To achieve higher efficiencies both the operating temperatures of materials (Fig. 5) have to be increased and more effective heat removal technologies have to be developed. Some of these technologies are discussed in the following section.

3.5. High heat flux removal technologies for divertors and blankets

3.5.1. ITER divertor

In steady state, about 20% of the fusion energy produced must be removed from the reactor through the divertor targets. Here the fusion ions, unburnt fuel, and impurities from plasma–wall interactions deposit their kinetic energies and are then removed at low velocities. The ITER's divertor (ITER, 2002) consists of 54 cassettes, where each cassette consists of inner and outer vertical targets, a dome, openings for removing the particles by vacuum pumps, and a backbone structure which houses the manifolds for the coolant (Fig. 10). The upper regions of inner and outer vertical targets are covered with tungsten monoblocks and the lower regions with carbon-fibre composite (CFC). The dome and the reflector plates are covered with tungsten monoblocks. The monoblocks are staked on water-cooled tubes manufactured from a high thermal conductivity heat sink copper alloy Cu–Cr–Zr (0.5–1.2 wt%Cr, 0.03–0.3 wt%Zr, rest Cu) and the divertor structure is made from the RAFM steel. The W monoblocks are designed to remove up to 5 MW/m^2 steady-state and 10 MW/m^2 (2s) transient, and the CFC monoblocks up to 10 MW/m^2 steady-state and 20 MW/m^2 (10 s) transient, heat flux loads (Herrmann et al., 2011; Pitts et al., 2011). The monoblocks vary in size (about 30 mm wide and high and 10–20 mm wide) and together with the cooling tubes (equipped with twisted tape inserts) are designed to operate within their operating temperature windows and avoid the critical heat flux of the coolant with a margin of 1.4 (Raffray et al., 1999b; Ibbot et al., 2001). Water enters into the cooling tubes at about 100 °C and 4 MPa by first

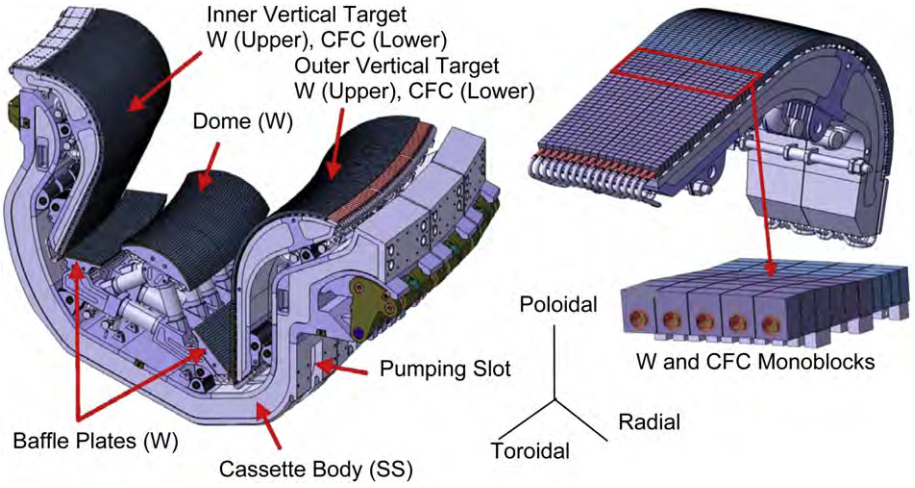

Fig. 10. The ITER's divertor consists of 54 cassettes (each about 5 m long, 2 m high, 0.5–1 m wide) whose plasma facing surfaces are covered with tungsten and carbon-fibre composite monoblocks (ITER, 2002).

flowing through the CFC targets (where the heat fluxes are the highest) and then through the tungsten targets (where the heat flux loadings are smaller). The divertor armors are expected to operate at high temperatures (700–1000 °C) and be replaced periodically (1–2 years) due to the high rates of erosion of these components (ITER, 2002).

Alternate divertor designs are being considered for DEMO reactors that can safely remove much more heat than the standard divertor employed in ITER. The safe exhaust of this huge power, without destroying the divertor target plates and damaging the quality of plasma, is a serious design challenge that requires the development of different high performance energy conversion schemes for divertor targets (see the following sections) and different divertor concepts. One such concept is the super X-divertor, whereby the plasma-wetted area is increased by employing an extra X-point which puts the divertor plates at the largest major radius possible inside the toroidal magnetic field coils (Valanju et al., 2010). The consequences of this design are that the divertor targets operate with lower heat fluxes (5 MW/m^2) and temperatures.

3.5.2. Flat-plate, T-tube, finger, and copper-SiC fibre composite heat removal schemes

Copper and steels are not suitable at high temperatures that are required for achieving high thermal conversion efficiencies, and water as a coolant is undesirable where there is a possibility of contact with Be and liquid metals. Use of water at subcritical conditions would also waste 10–20% of the available energy. Conditions appropriate for DEMOs are high operating temperatures, robustness and lifetime of heat removal components, and integration of heat removal and tritium breeding within the blankets. These requirements make He a very useful coolant and several technologies are being developed that use this coolant with the refractory metal tungsten. The promising concepts employ high velocity He-jets and He flowing through the porous media, both of which can be employed for cooling of blanket and divertor armors.

An abrupt change of momentum of a high velocity He jet causes a large turbulence increase and a corresponding increase in heat transfer coefficient. This concept can remove in excess of 10 MW/m^2 of heat and has been built into the plate-type-, T-tube-, and finger-type configurations, or into a combination of these configurations (Norajitra et al., 2005; Nygren et al., 2011; Tillack et al., 2011). The plate-type configuration (Fig. 11) is made of 1 m long poloidal and nine 20 cm wide toroidal channels, each of which consists of supply and return He headers. A high pressure (10 MPa) and velocity (258 m/s) He jet from the supply header impinges on the underside of the 5-mm thick castellated W armor of the plate where it is heated from 600 to 777 °C by removing 10 MW/m^2 of surface heat flux and 17.5 MW/m^3 of volumetric heat rate, while maintaining the material limits of stress (500 MPa), temperature (1300 °C), and pumping power (<10% of the heat load). The ITER's divertor area of 150 m^2 would require some 750 plate-type units (Tillack et al., 2011).

The T-tube design also employs the high velocity and pressure jet concept, whereby the He inlet and outlet headers are placed close together at the center of a heat sink (Fig. 12) (Ihli et al., 2007; Tillack et al., 2011). The high velocity jets striking the upper surface of the outer tube are very effective for removing 10 MW/m^2 heat loads while maintaining the stress and temperature limits of tungsten armor as in the plate-type configuration. He is supplied at 10 MPa and 600 °C and exits at 700 °C. About 110,000 T-tubes would be required to cool 150 m^2 of the divertor area of ITER (Tillack et al., 2011). T-tubes reduce both the thermal fatigue and the reliability of the divertor as compared to the plate-type configuration.

A further reduction of divertor thermal stresses (and reduction of cooling system reliability) can be accomplished with a modular divertor constructed from He-cooled finger modules (Fig. 13) (Norajitra et al., 2010; Končar et al., 2011; Nygren et al., 2011; Tillack et al., 2011). Here, a nine-finger module consists of nine fingers arranged into a cooling unit. Each finger is covered with a tungsten tile and connected to a WL10 (99°wt%W, 1 wt% La_2O_3) timble which is cooled by high velocity He jets (150–200 m/s) issuing from the cartridge that supplies the coolant. The thermal load from the tile–timble combination is removed with the high pressure (10 MPa) He entering at 600 °C and exiting at 700 °C. Results from the tests of this concept show that some fingers can withstand heat loads in excess of 10 MW/m^2 for as many as 1000 cycles and still remain within the stress and temperature limits of finger materials. A divertor of 150 m^2 requires some 535,000 fingers, which calls for a very high reliability of these units to keep the divertor functional without servicing.

The size, number, and arrangement of jets on a cartridge influence the pressure drop, heat transfer, and thermal stress performance of the finger. A compromise of these characteristics is necessary to achieve the best design, and different cartridge

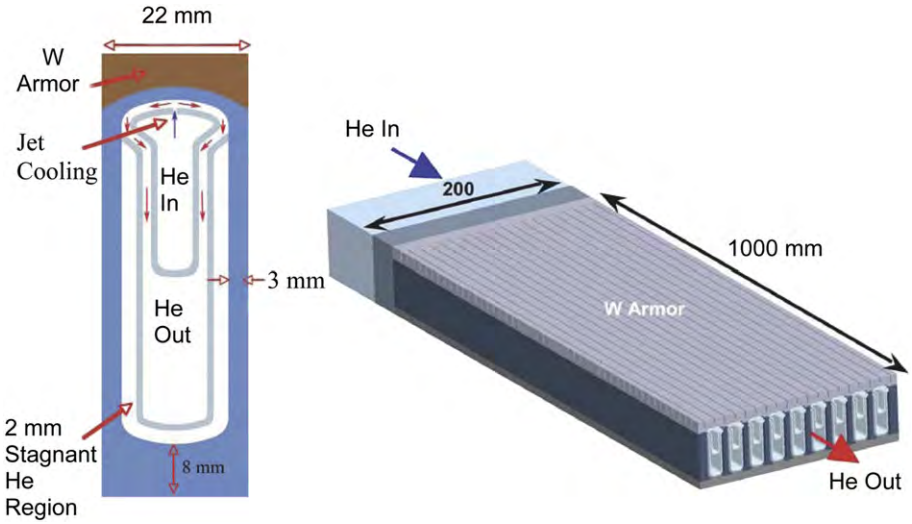

Fig. 11. The plate-type configuration (right) is made of castellated W armor blocks mounted on He-cooled channels. High velocity helium jets (left) cool the underside of the module's armor and produce large heat transfer coefficients (Nygren et al., 2011). ©2011 Elsevier, reproduced with permission.

designs have been evaluated for this purpose (Hermsmeyer and Malang, 2002). The design with 25 holes, arranged one in the center and the rest in four rows, with each hole having the diameter of 0.6 mm, produces a very good heat transfer performance and an acceptable pumping power and thermal stresses.

Common to the plate-type, T-tube, and finger configurations is the use of W tiles as thermal and sacrificial shield against high heat fluxes. The tungsten alloy WL10 extends the operating temperature window of W to 1300 °C. Small structures such as fingers have lower thermal stresses than bigger structures, but many of such units covering the divertor surface can render the divertor very unreliable. This design issue and that associated with neutron irradiation of modular designs have not yet been addressed.

High thermal conductivity materials such as copper and its alloys can remove large heat fluxes, but they cannot withstand temperatures above about 350 °C. However, a composite made of copper reinforced with 140 μm SiC fibres can withstand even 550 °C under neutron irradiation and can be employed for some of the chamber wall components of the reactor (Brendel et al., 2004). Fig. 14 illustrates a design where such a composite forms the first wall of a heat sink through which circulates a coolant to remove the heat.

3.5.3. He-cooled porous matrix heat removal concepts

Heat removal at high temperatures (600–1500 °C) demands refractory materials, but these materials are brittle at low temperatures and suffer from recrystallization and thermally induced stress cracking at high temperatures. Fabrication of refractory materials is also challenging. Their integration into the porous media concepts offers, however, the possibility of producing structures with very high heat transfer performance and Fig. 15 illustrates some of these designs.

The concept shown in Fig. 15a involves a two-tube structure. This is surrounded by a porous matrix annulus which is imbedded into a heated metal block covered with a refractory metal erosion surface. High pressure and temperature helium at 10 MPa and 640 °C enters the inner metal tube and exits along the longitudinal slot on the upper surface of the tube. It then flows along the circumference of the porous annulus where it is heated from the heat stored in the block and porous annulus and exits at 740 °C

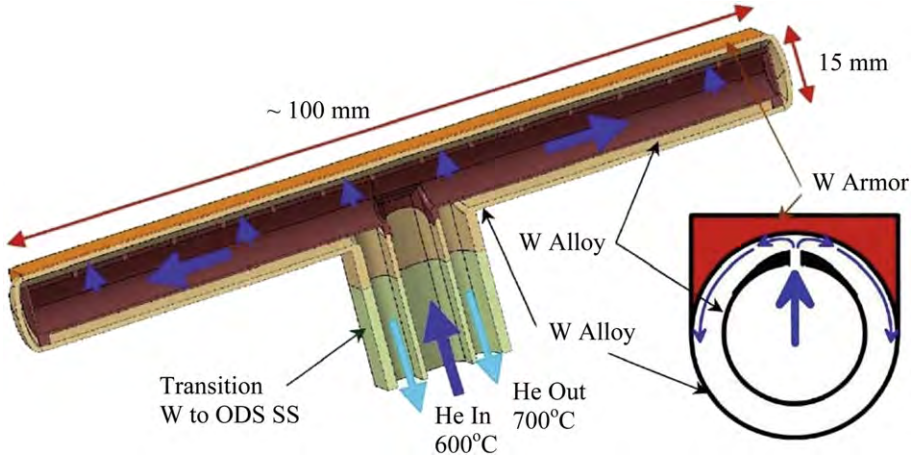

Fig. 12. In the T-tube cartridge of a divertor design (Tillack et al., 2011; Ihli et al., 2007), He from the inner tube of a central manifold flows into the 1 mm thick inner tube of the cartridge and exits through 0.5 mm holes at the top of the tube. High velocity jets impinge on the underside of a concentric outer tube covered with W armor. Heat is removed through this tube and the outer tube of the central manifold. ©2007, 2011, Elsevier, reproduced with permission.

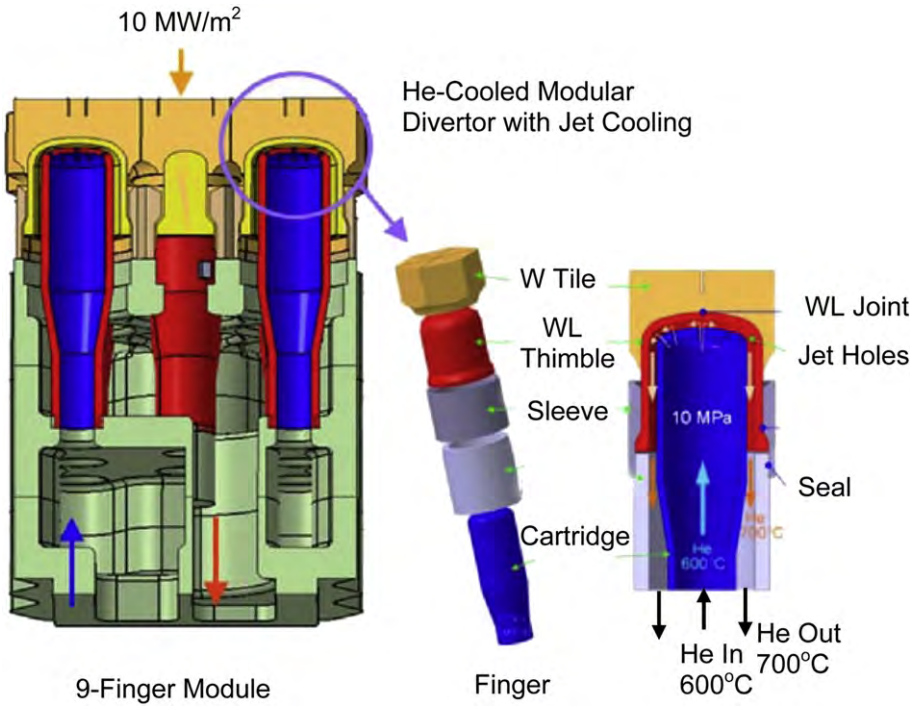

Fig. 13. A highly modular divertor consists of many small modules, each of which employs about a dozen of 15 mm diameter He-cooled fingers. Shown in the illustration is the nine-finger module which incorporates nine fingers cooled by high velocity He jets (Norajitra et al., 2010). ©2010 Elsevier, reproduced with permission.

through a longitudinal slot on the bottom of outer tube. The heat transfer performance of this configuration is 10 MW/m^2 (Hermsmeyer and Malang, 2002).

The design in Fig. 15b is a variation of the design of Fig. 15a. Here the coolant flows through the porous medium around the circumference of the tube and not along the length of the (150 cm long) tube (Pulsifer and Raffray, 2002). When this device is operated with the inlet He temperature of 550 °C, pressure of 4 MPa, and heat load of 5 MW/m^2 it produces a 150 °C temperature drop through the 3 mm thick W armor and thus an acceptable operation within the allowable temperature window of tungsten. The 30 MW/m^2 heat flux requires, however, a 900 °C temperature drop that is outside of this window and thus not acceptable, unless very low porosity and very high pressure drop or 1 mm thick W armor, are employed.

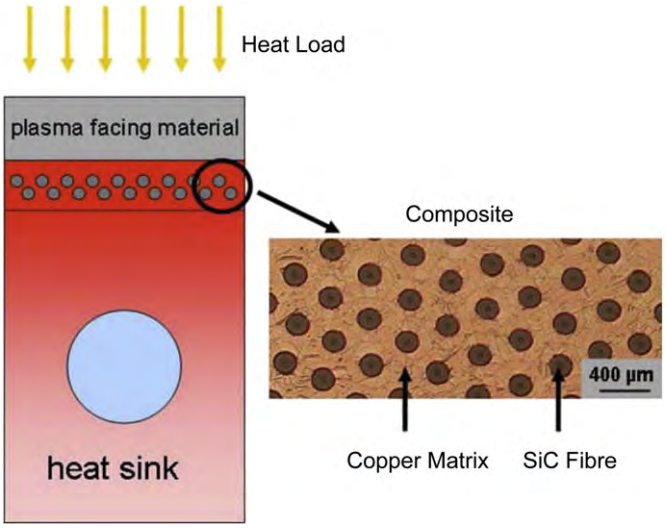

Fig. 14. Heat sink incorporating a composite layer made of copper and SiC fibres as the plasma facing material (Brendel et al., 2004). ©2004 Elsevier, reproduced with permission.

The dual-channel porous metal heat exchanger module shown in Fig. 15c consists of a tungsten cylindrical cup containing a hemispherical shell of brazed tungsten porous metal. The cup is brazed onto a tungsten cylindrical tube containing stainless steel bellows for He supply and return, and a plug seals the inner hemispherical surface of porous metal. Helium flows into the 25 mm diameter module and enters the porous metal shell at the bottom. The coolant then flows on the outside of the porous metal and is collected at the top of the shell and then discharged from the module through a stainless steel tube. Tests of the module with He at 4 MPa show that 5.9 MW/m^2 can be removed with the maximum surface temperature of 840 °C and helium temperature rise of 200 °C (Youchison and North, 2001).

The porous foam-in-tube concept employs axial flow in a W tube (Fig. 15d), whereby the foam ligaments function as a very effective fin and turbulence promoter. Tests of this concept show that He at 4 MPa can absorb 22.4 MW/m^2 at the peak tube surface temperature of 2300 °C and 10 MW/m^2 at 1500 °C, with relatively low pressure drops. At 3 MPa, 2 MPa, and 1 MPa, the porous foam-in-tube can remove surface heating loads of 12 MW/m^2, 9.5 MW/m^2, and 5.7 MW/m^2, respectively, which is impressive. The axial flow of coolant in the foam-in-tube concept has, however, the drawbacks of large pressure drops, onset of instabilities when the flows in tubes are arranged in parallel, and a sharp drop in heat transfer coefficient over a small length. This produces uneven surface temperatures and large thermal stresses in materials (Youchison et al., 2007).

The short flow path foam-in-tube concept (Sharafat et al., 2007) (Fig. 15e) has, however, a better performance, because the flow path length through the porous medium is minimized. This concept incorporates two concentric W tubes, with a tungsten foam

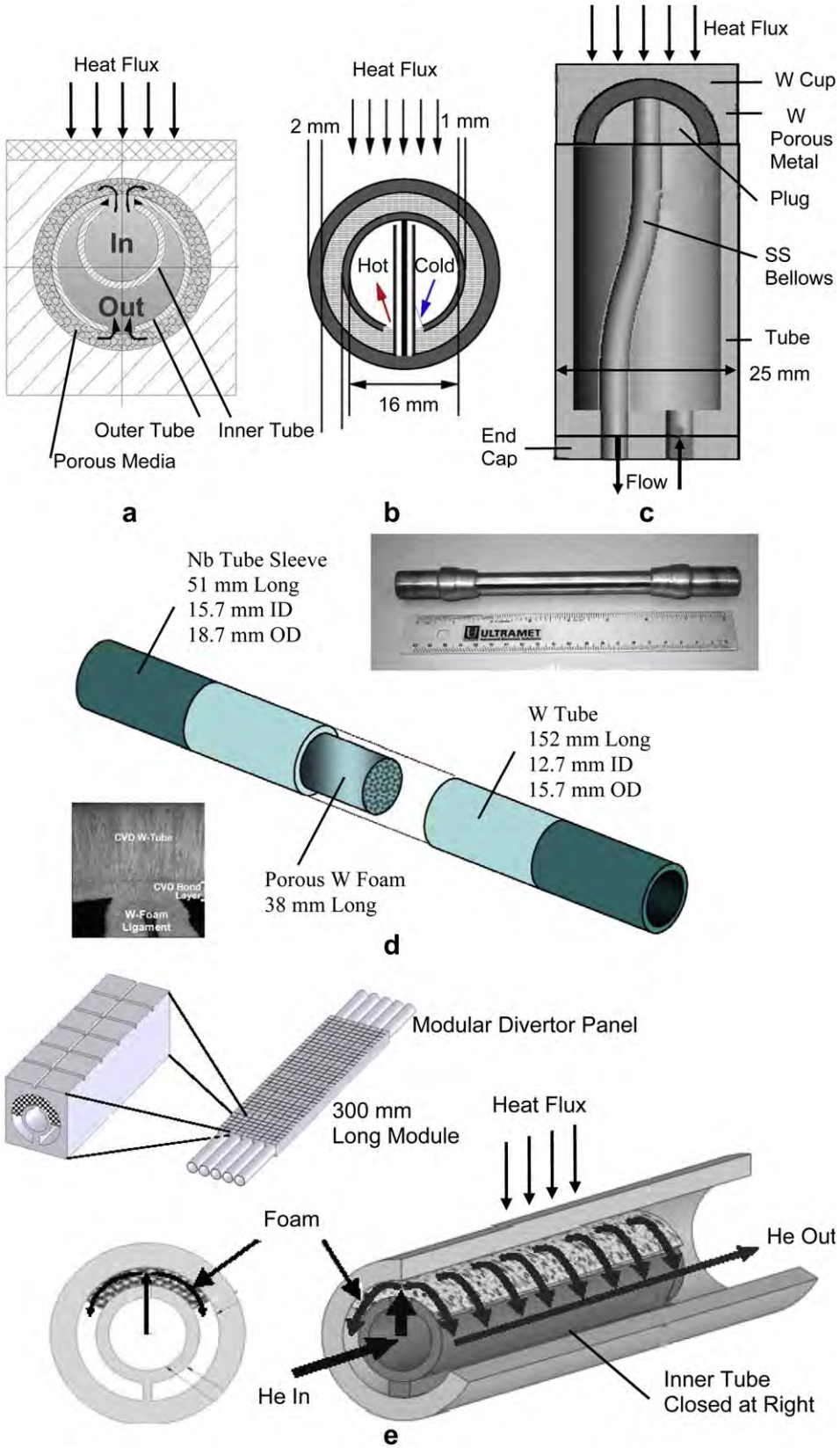

Fig. 15. Helium-cooled porous media heat removal configurations. (a) Two-tube with porous annulus configuration (Hermsmeyer and Malang, 2002). (b) Variation of two-tube configuration (Pulsifer and Raffray, 2002). (c) Dual-channel porous metal heat exchanger concept (Youchison and North, 2001). (d) Porous foam-in-tube concept (Sharafat et al., 2007; Youchison et al., 2007; Tillack et al., 2011). (e) Short flow path foam-in-tube concept (Sharafat et al., 2007). As shown in the upper left of (e), the individual W foam/W tube channels can be integrated into the blanket and divertor modules. ©2002, 2007, 2011 Elsevier, reproduced with permission.

partially sandwiched between them. The W foam heat exchanger is selectively located to minimize the flow path length and thus the pressure drop, which maximizes the heat transfer performance and maintains a near-uniform temperature over a large surface area of the device. The 14 mm OD inner tube contains a 4 mm wide slot for supplying He at 327 °C and 150 kPa. Analysis shows that the pressure drop is almost independent of the tube length and more than an order of magnitude smaller than in the foam-in-tube concept. No experimental performance of this design appears to be available.

3.5.4. Heat removal concepts with enhanced critical heat fluxes

The coolant's capability to remove heat from a heat transfer surface is measured by its critical heat flux (CHF) (point C on the Nukiyama's boiling curve in Fig. 16a). CHF depends both on the properties of the coolant and on the geometry of the heat transfer surface, and various flow configurations have been proposed to increase this limit while maintaining reasonable pumping power requirements (<10% of CHF). Twisted tape inserts in round tubes, hypervapotron for rectangular channels, and helically coiled wire and grooved tubes (Fig. 16b) are some typical CHF enhancement concepts (Chang and Baek, 2003), but only the first two techniques have received attention for cooling of fusion reactors (Baxi, 1995; Escourbiac et al., 2005; Escourbiac, 2008). CHF in tubes with tape and wire inserts and grooves occurs without the transition boiling, but not in hypervapotrons.

Hypervapotron is a channel-like device with internal fins machined inside the channel and oriented perpendicular to the flow of coolant through the channel. The local CHF is avoided by the conduction of excess heat into other parts of the fins where single-phase flow and/or nucleate boiling can safely convect the heat away. This allows the device to operate at higher than local CHF and within the transition boiling regime without experiencing the burnout or excessive surface temperatures. It appears that a fin aspect ratio of 4/3 gives the best heat transfer performance (Milnes, 2010). The hypervapotron test module considered for cooling of ITER's divertor (Fig. 17) consists of the Cu–Cr–Zr heat sink (741 mm long and 27 mm wide) that is armored with 25 flat CFC tiles (18.5 mm long and 6 mm wide) and cooled by water. A cyclic (1000 cycles, each lasting 10 s) testing of this module demonstrated that it can handle heat loads of 25 MW/m^2 and surface temperature of 1500 °C without experiencing the CHF limit or exceeding the thermal fatigue stress limit. The actual CHF for this module exceeds 30 MW/m^2 (Escourbiac et al., 2005).

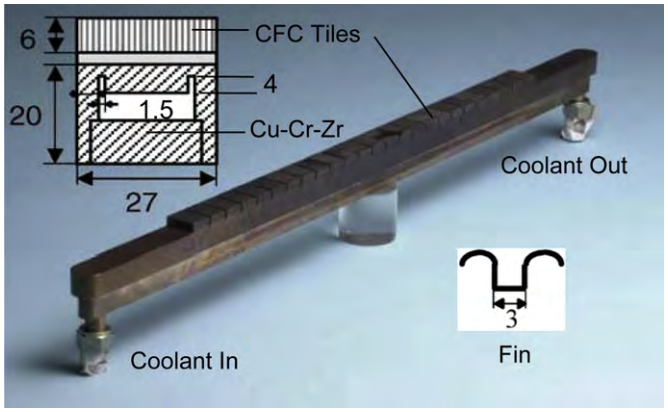

Fig. 17. Illustration of a hypervapotron module with the dimensions given in mm (Escourbiac et al., 2005). Cross-section of the module shows 4 mm deep and 3 mm wide fins separated from the sides of the channel with 1.5 mm grooves running along the length of the channel. ©2005 Elsevier, reproduced with permission.

3.5.5. Liquid metal and molten salt films and capillary pore systems as first walls

Heat removal from fusion reactors with liquid films forming the first walls is attractive for several reasons. Liquid metals and molten

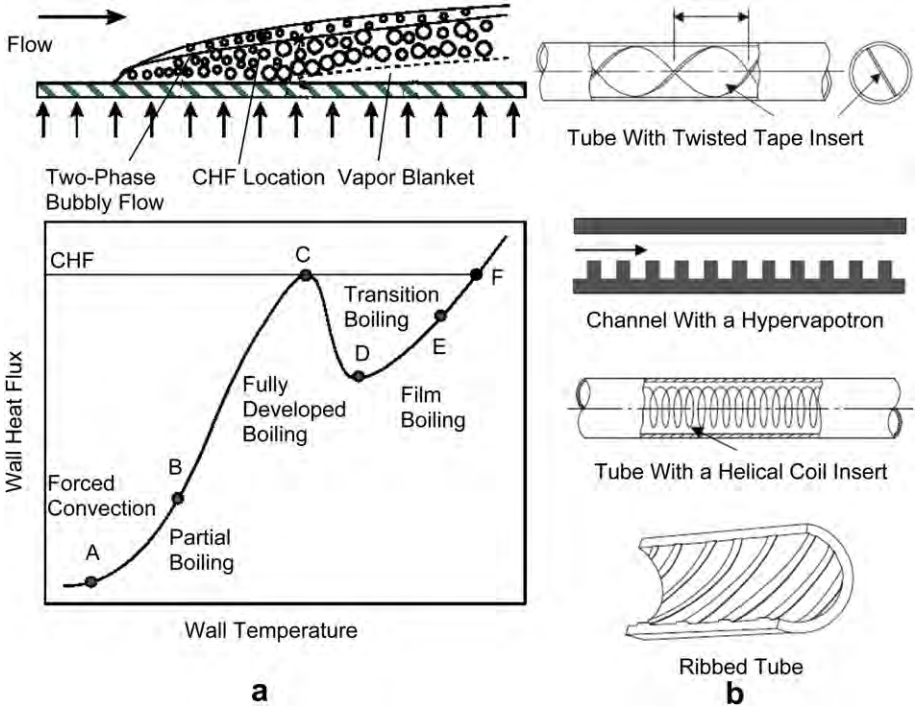

Fig. 16. (a) Nukiyama's boiling curve. As the heat flux increases beyond the critical heat flux (CHF) at point C, the surface temperature increases abruptly to point F, because of the heat transfer resistant vapor blanket between the surface and subcooled liquid. (b) Various geometries employed to increase the CHF limit. Adapted from Chang and Baek (2003).

salts can remove large quantities of heat at high temperatures, which is necessary to obtain high thermal conversion efficiencies. When they are used as first wall and divertor target materials, they can reduce erosion and neutron irradiation drawbacks of tungsten and CFC composites and may thus lessen the important maintenance problem of these components. Important issues with liquid metals PFCs are, however, the difficulties with liquid metal supply and removal, MHD behavior under the spatially varying magnetic field environment, chemical reactivity, and plasma contamination. Lithium, gallium, tin, lithium-thin, flibe, and flinabe are some promising candidates for PFCs and some of their properties are summarized in Table 3. The practical operating temperature windows of these materials are determined by the pressure of the reactor's vacuum chamber, which can vary between 10^{-7} and 10^{-1} Pa during a typical cycle of fusion plasma burn and removal of ions and impurities from the chamber (Stacey, 2010). All coolants except Li and its compounds require the neutron multiplier beryllium to increase the tritium breeding ratio beyond the minimally accepted value of 1.05. Some clear advantages of using Li–Sn over either L or Li–Pb as the first wall material are its relatively high operating temperature window and electrical resistivity.

Compared to Ga and Sn, Li has the largest heat capacity and lowest atomic number and temperature at which the vapor is in equilibrium with liquid at fusion reactor vacuum vessel relevant operating pressures (10^{-7} to 10^{-4} torr). Lithium's practical operating temperature limit of around 300 °C is low because it rapidly evaporates above this limit, whereas Ga, Sn, Li–Sn, flibe, and flinabe have much better temperature limits (600–1000 °C) that are useful for achieving high energy conversion efficiencies. Lithium has a good capacity for collecting plasma ions and impurities and separating hydrogen isotopes from helium in the pumping system (Mirnov, 2009). The highest tolerance for the evaporative flux is the divertor and this is where Li can be used most effectively (Majeski, 2010). Lithium is the most and gallium the least chemically aggressive of the three metals. Gallium alloys with many metals and does not readily attack ceramics, whereas tin is compatible with refractories. Lithium is also compatible with refractories, stainless steel, vanadium, and niobium, but not with ceramics above 400 °C. Most refractory metals are compatible with Sn up to about 1000 °C, Nb is compatible up to 850 °C, and V up to 700 °C. Li–Sn is compatible with Ta up to 1200 °C. Sodium has a high vapor pressure and cannot be used as a PFC, but it can be employed as an effective coolant of blankets and divertors (Golubchikov et al., 1996; Mirnov, 2009; Majeski, 2010).

Liquid metals can be used in various configurations to protect plasma facing components of the reactor, such as: Liquid metal walls, liquid curtains, liquid capillary pore systems, forced convection subcooled boiling, natural convection evaporation, heat pipes, and thermosyphons. The first three configurations involve the use of liquid metal's sensible heat and the remaining its latent heat for cooling of fusion reactors. The reactor configurations employing Li are the most developed and several tokamak designs employ this metal for both, wall conditioning and as the first wall coolant (Mirnov, 2009; Majeski, 2010; Majeski et al., 2010). Although Ga and Sn provide much less restrictive operating temperature limits than lithium, these metals have not yet been adequately investigated for applications to fusion reactors.

The APEX Team identified lithium, tin, tin–lithium, lead–lithium, gallium, flibe, and flinabe as viable candidates for liquid walls facing plasma and flowing along the inboard and outboard surfaces of fusion reactor chamber walls (Fig. 18) (Abdou and The APEX Team, 2001; Nygren et al., 2003; Abdou et al., 2005). As noted above, the attraction of this concept is that the first wall liquid surface is continuously renewed and can be largely immune to both radiation damage and thermal stresses that normally affect and limit the performance of a solid first wall. Both thin (1–2 cm) and thick (>40 cm) liquid walls can remove heat fluxes in excess of 20 MW/m^2. A thick liquid film is more effective for attenuating neutrons than a thin film and thus better for reducing the radiation damage, but establishing a stable thick film flow appears to be a major issue of this design. In the gravity-momentum driven concept, a liquid coolant is injected at 10 m/s at the top of the chamber with both tangential and azimuthal angles to provide the necessary adherence of liquid to the curved surface of the reactor chamber. In the electromagnetically restraint concept, the liquid metal adherence is achieved by the electromagnetic force produced by a flowing electric current in the liquid. Liquid lithium walls provide the advantages of high power densities (1 GW/m^2 was measured with a lithium flow of 20 m/s without Li boiling (Nakamura et al., 2003)), improved plasma stability, reduced erosion and thermal and mechanical stresses of the blanket, reduced volume of radioactive waste, and long lifetime of chamber wall materials. The key issues are plasma-liquid and liquid metal–wall interactions, stability of liquid wall under plasma disruptions, MHD effects associated with liquid metals in contact with electrically conducting walls, liquid surface temperature and evaporation control, and accumulation of lithium in plasma from splashing. Lithium and flibe designs have problems with the excessive production of impurities within the plasma outside of their operating temperature windows. Tin with the operating temperature window of 800–1000 °C for the first wall and as high as 1600 °C for the divertor targets provides a more acceptable performance of plasma–wall interactions than lithium, but lithium is better for recycling hydrogen isotopes and helium ash within its (low) operating temperature window. A flinabe liquid wall operating at 500 °C and in turbulent flow regime produces minimal MHD effects and can remove up to 12 MW/m^2 heat loads in the divertor. When also used as the coolant of the blanket (Fig. 18b), the flinabe's exit blanket temperature of 650 °C offers the possibility of producing thermal conversion efficiencies of about 50% (Nygren et al., 2003). One disadvantage of flinabe is its poor tritium breeding ratio, which requires that it be used with beryllium to achieve an acceptable ratio.

Some of the problems with continuous liquid metal films can be reduced or eliminated with jet-drop curtains (whereby the liquid metal flow is broken into 2–4 mm droplet streams flowing along the inner metal wall of the blanket) and with liquid metals flowing in capillary pore systems integrated into the plasma facing surfaces of blankets and divertors (Golubchikov et al., 1996; Abdou, 2007b; Mirnov and Evtikhin, 2006; Mirnov, 2009). Lithium capillary pore systems (LiCPS) manufactured from 30 to 160 μm stainless steel, Mo, V, and W grids employ a slow moving (<1 cm/s) Li as the working fluid operating at temperatures below 600 °C (Mirnov, 2009; Lyublinski et al., 2010). Lithium confinement, redistribution, feeding, and surface stabilization in these systems depend on the capillary pressure $P_c \sim 1/R$, where the liquid meniscus radius R depends on the capillary channel's pore radius and incident heat flux. Capillary pore systems work well with lithium because of its ability to wet the solid and produce high capillary pressures. LiCPS have been subjected to magnetic fields up to 6 T, steady-state heat fluxes up to 25 MW/m^2, and transient (several milliseconds) fluxes exceeding 10 GW/m^2, without causing catastrophic events leading to Li injection into the plasma. The erosion of a LiCPS surface (up to 100 μm per pulse) is suppressed by almost two orders of magnitude in comparison to the erosion of a free lithium surface (Vertkov et al., 2007). The erosion (evaporation) of Li from CPS increases with temperature, but the consequences of this drawback have not yet been assessed.

Fig. 19a illustrates mock-ups of Mo and SS meshes with pore sizes of 30–150 μm for testing within the lithium operating temperature window and heat fluxes up to 5 MW/m^2. Stainless

steel is not suitable at high temperatures and heat fluxes and a new CPS mat from tungsten fibres with diameters of 30 μm and pore radii of 15 μm was developed for testing in tokamak fusion reactors (Fig. 19b). Both the strength and the thermal conductivity of the tungsten structure are almost an order of magnitude higher than those of stainless steel (Lyublinski et al., 2010).

LiCPS are designed for integration into the plasma facing walls of blanket and divertor modules from where the heat must be efficiently removed. Cooling of LiCPS with water is not recommended and cooling with Na, Na–K eutectic alloy, Li, or some other suitable high thermal capacity coolant and heat exchanger surface combinations, is much more acceptable. Loss of lithium from erosion,

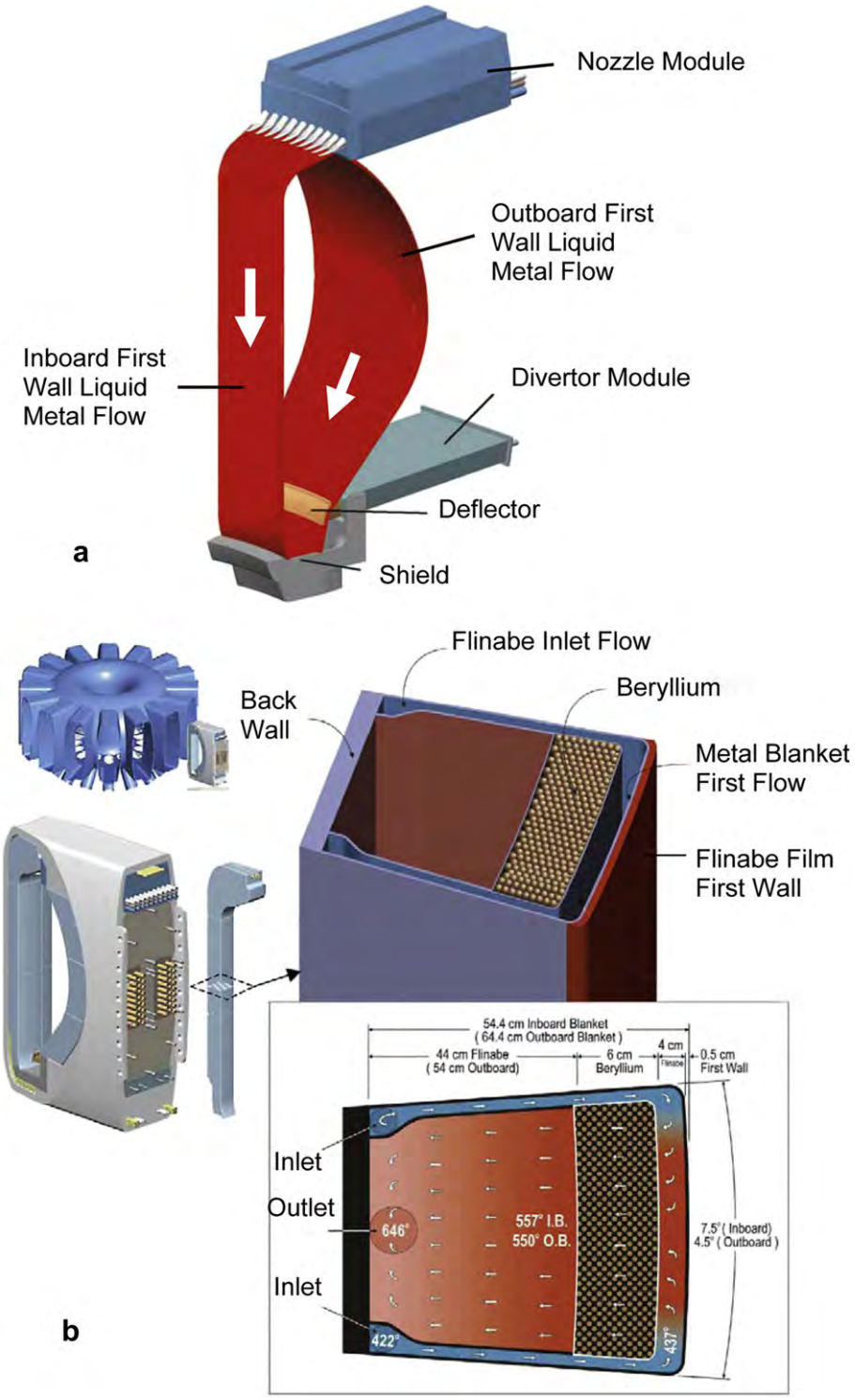

Fig. 18. Liquid film first wall concept (Nygren et al., 2003). (a) Each interlocking module consists of a nozzle module with "self-shielding" nozzles for producing inboard and outboard liquid films and a divertor module with a deflector for promoting mixing and directing liquid streams into the coolant and plasma ash collectors. (b) Flinabe flows along the plasma facing metal wall and through the interior of the blanket. The chamber of this ARIES-RS fusion reactor has the major radius of 5.5 m and aspect ratio of 4, and was designed to produce 4 GW of fusion power. The plasma is confined with 16 toroidal field coils surrounding the chamber.

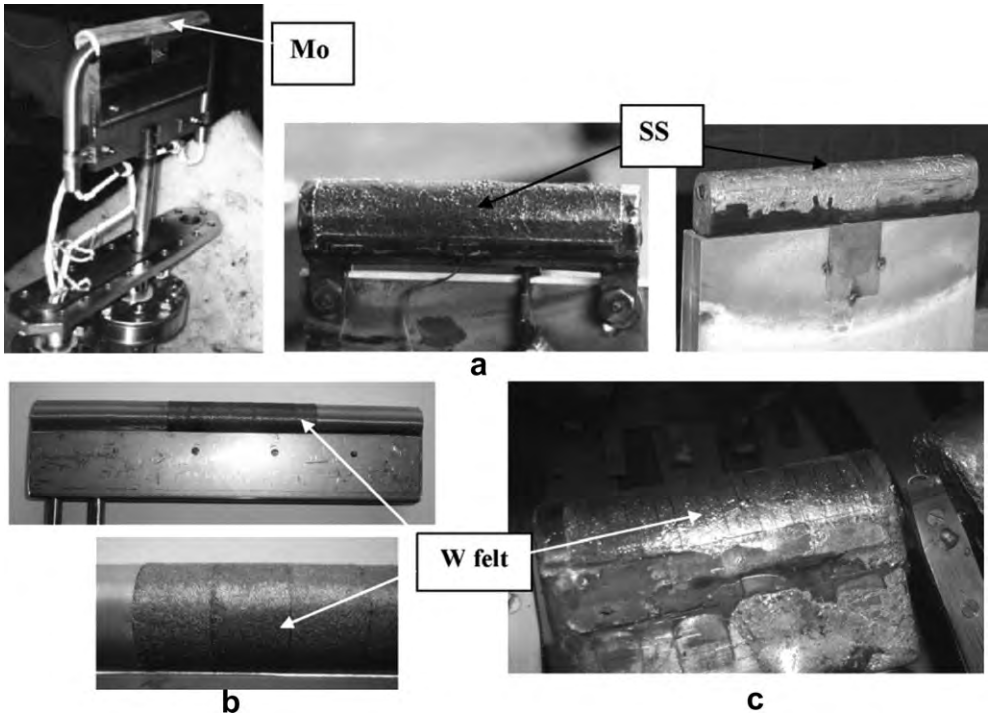

Fig. 19. LiCPS mock-ups developed in Russia for use in divertor and blanket modules. (a) A slow moving lithium circulates through Mo and stainless steel meshes. (b) 1 mm-thick CPS mats manufactured from tungsten fibres (Lyublinski et al., 2010). (c) W felt after the test. ©2010 Elsevier, reproduced with permission.

tritium breeding, and separation of hydrogen isotopes and helium from lithium requires the appropriate lithium feeding, tritium extraction, and impurities separation systems (Mirnov, 2009; Vertkov et al., 2007). Several experimental tokamaks (in Italy, Russia, and US) with liquid lithium PFCs operated successfully during the past decade and the hopes are high that the lithium screening effect can serve as a basis for the design of PFCs in tokamaks (Mirnov, 2009). But (as we noted above), Li has a low operating temperature window when employed as a PFC and will not be suitable for use in this capacity in DEMOs and subsequent commercial fusion reactors.

Some experiments using liquid gallium jets as a PFC and operating at about 700 °C show no severe effects of this coolant on plasma performance (Gomes et al., 2008). Other experiments conducted with weak magnetic fields (about 0.1 T) and thin films (2–3 mm) of eutectic of gallium, indium, and tin (67 wt% Ga, 20.5 wt% In, 12.5 wt% Sn) show that the initial flow velocity of the metal stream flowing perpendicularly to the applied magnetic field can produce unwanted effects at both low and high velocities (Narula et al., 2006). At low film velocities (typically 1 m/s), the film exhibits a ten-fold increase of thickness (and consequently a ten-fold reduction of its velocity downstream of the jump), and at higher velocities (about 3 m/s) the film is pushed away from the sidewalls of the conducting channel. Both of these effects are detrimental and suggest that an appropriate compromise between the operating parameters of liquid metal films and magnetic field environment must be found before this design strategy can be employed in fusion reactor systems.

3.5.6. Heat removal with evaporating liquid metals

At 181 °C, the heat of vaporization of lithium (22.6 MJ/kg) is ten times higher than that of water at atmospheric conditions. This suggests that the evaporating lithium can be used to remove high heat loads from the reactor and several interesting designs have been proposed for this purpose. Here we will discuss the tube-tray (Abdou and The APEX Team, 2001) and the heat pipe arrangements (Carlson and Hoffman, 1972; Werner and Hoffman, 1983; Dobran, 1989; Kovalenko et al., 1995; Makhankov et al., 1998).

In the tube-tray configuration (Fig. 20), liquid lithium at 1200 °C and 0.035 MPa is evaporated in 3 m long first wall tubes arranged along the toroidal direction of the reactor and joined together to contain the Li vapor in the blanket (Fig. 20b). Placed within each 4 cm diameter tube is another tube which supplies liquid lithium to the porous layer on the inside of the outer first wall tube. Here the liquid is vaporized (as in a heat pipe) and the vapor is collected in the blanket. The neutron-generated heat in the blanket evaporates the liquid lithium in poloidally arranged trays from where the vapor is separated from the liquid and also collected in the blanket. The vapor in the blanket is condensed by transferring heat to a high pressure helium operating in Brayton cycle. The condensed Li vapor is then pumped back to the inner tubes and trays (Fig. 20a). Many details of this heat removal concept have not yet been worked out, but the projection is that this design can remove surface heat loads of 2 MW/m^2 and neutron loads of 10 MW/m^2 (Abdou and The APEX Team, 2001). The refractory metal alloys and Sic/SiC$_f$ composites are currently the only acceptable materials for constructing the blanket of such a reactor.

A heat pipe employs the latent heat of its working fluid to transport heat from one region of the device to another. The working fluid evaporates in the evaporator of the pipe and the vapor moves toward the condenser of the pipe where it is condensed by transferring heat to a secondary coolant. Capillary forces in the wick within the pipe move the liquid from the condenser to the evaporator. The heat transfer process in heat pipes is nearly isothermal, which allows the device to operate at reduced thermal stress levels. Heat pipes incorporate a variety of designs which optimize the circulations of working fluids (Dobran et al., 1987) and are usually constructed from tubes of various lengths and diameters, filled with working fluids, and then closed at both ends (Reay and Kew, 2006). The working fluids of heat pipes are chosen on the basis of operating

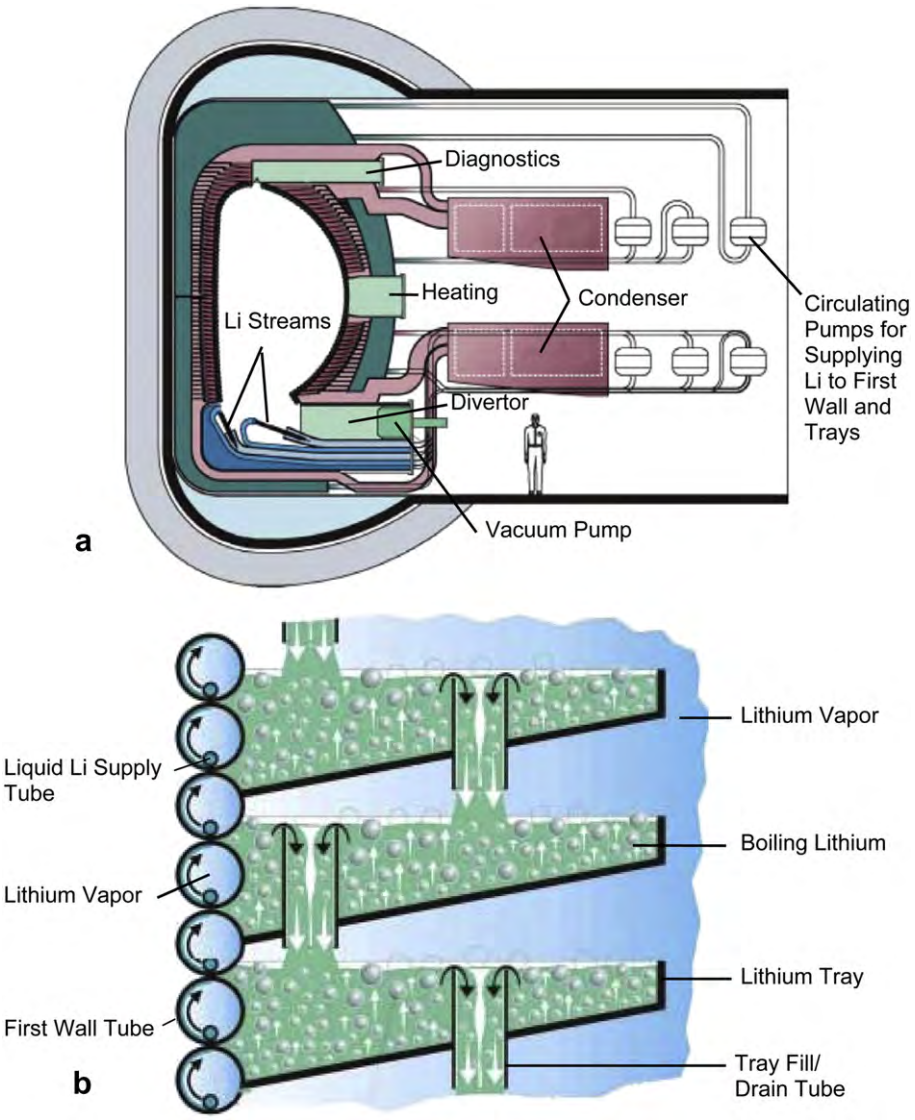

Fig. 20. (a) Cross-sectional view of the EVOLVE (evaporation of lithium and vapor extraction) heat removal concept. (b) Schematic of heat removal by evaporation and boiling of Li at 1200 °C and 0.035 MPa (Abdou and The APEX Team, 2001). ©2001 Elsevier, reproduced with permission.

temperature and heat transfer requirements, and as Table 4 shows water and liquid metals Li, Na, K, and Cs provide large temperature windows for applications to fusion reactors. The maximum heat fluxes in this table correspond to the coolants' heat transport capacities and not to the (lower) heat fluxes that can be practically transferred through the evaporator and condenser surfaces of heat pipes. The effective thermal conductivity of lithium is 10^4 times larger than that of copper and is the most effective for transporting heat at high temperatures. Its low density permits high flow velocities without encountering high pressure drops and reaching its operating limits (see below). All liquid metals in the table are chemically active with oxygen compounds and require special structural materials for containment and wick structures, such as nickel, molybdenum, niobium, and tungsten alloys. Thermacore Inc. (DATASHEET, 2008) claims that one of its lithium heat pipes operated at heat loads of 1.26 GW/m^2 and that its sodium heat pipe operated for 16 years without a failure.

Table 4
Operating temperatures and heat transport capacities of water and some liquid metals for heat pipe applications to fusion reactor technology (Vergaftik, 1975; Bystrov et al., 1990).

Working fluid	Temperature/pressure range (°C/Pa)	Heat of evaporation (kJ/kg)	Maximum heat flux (MW/m^2)
H_2O	$40–200/7.375 \times 10^3–1.5551 \times 10^6$	2173	5
Cs	$300–500/3.58 \times 10^2–1.51 \times 10^4$	527	15
K	$400–800/2.201 \times 10^3–1.54 \times 10^5$	2001	40
Na	$600–1000/3.741 \times 10^3–2.73 \times 10^5$	3972	80
Li	$1000–1700/5.157 \times 10^3–7.75 \times 10^5$	19,411	250

Heat transfer in heat pipes is limited by the countercurrent flow of liquid and vapor, wettability of channel and wick structures, sonic vapor speed, condensation limit, orientations of gravity and magnetic fields relative to the liquid flow direction, critical heat flux, and fluid viscosity (Dobran, 1987, 1989; Reay and Kew, 2006). These limits depend on the heat pipe's working fluid, operating temperature, wick geometry, structural materials employed, and external heat supply and removal configurations. Some of the effective ways to increase the heat pipe performance are by employing short length pipes, wicks with large pores, liquid return paths parallel to the magnetic field, low vapor velocities, low viscosity fluids, and fluids with large thermal capacities.

Heat pipes have been proposed for removing heat of ITER's PFCs, where the first wall temperatures are expected to remain below 350 °C. But the liquid metal heat pipes should be especially suited to DEMOs and subsequent generations of reactors operating at much higher coolant temperatures. The critical heat flux in a heat pipe increases with inclination and decreases with an increasing magnetic field perpendicular to the liquid flow direction (Carlson and Hoffman, 1972; Makhankov et al., 1998), because the liquid flow is either enhanced or inhibited, respectively. When the magnetic field is applied perpendicularly to the axis of a flattened cylindrical tube heat pipe it can remove 2–3 times more heat than a cylindrical heat pipe of the same cross-sectional area (Werner and Hoffman, 1983), and when a heat pipe is inclined it can transfer 20–50% more heat than in a horizontal position (Makhankov et al., 1998). Fig. 21 illustrates an integration of sodium heat pipes into different target zones of the divertor. Here the first level heat pipes serve to remove the heat from the divertor target areas and transfer it to the second level heat pipes from where the heat is removed by water-cooled tubes imbedded into the stainless steel structure of the divertor. It is claimed that such a Na heat pipe configuration can remove 3 MW/m^2 and Li heat pipe configuration 15 MW/m^2 heat loads. In another configuration, K, Na, and Cs heat pipes are integrated into 0.5 m wide and 1 m long blanket panels capable of removing about 1 MW/m^2 heat loads (Kovalenko et al., 1995).

A porous layer heat pipe concept employing Na and Li and operating at 875 °C (0.1 MPa) and 1200 °C (0.035 MPa), respectively, and capable of removing 5 MW/m^2 heat loads and 30 MW/m^3 of neutron-generated heat, is shown in Fig. 22 (Reimann et al., 2001). Liquid from an inner feed pipe is distributed through short tubes into a shallow and subcooled liquid metal pool. The heated porous layer of the device evaporates the liquid from the pool and the vapor is collected into the cylindrical cavity containing the feed pipe. The vapor is then condensed by a high pressure He (not shown) and the condensate is fed to the inner feed pipe and liquid pool. The MHD pressure drop of liquid metal is controlled by keeping the liquid speed below 0.1 m/s or 30% of its sonic speed. This configuration produces the thermal conversion efficiency of 57%, because it incorporates good heat pipe design strategies: Orienting condenser close to the evaporator, preventing boiling in the wick structure, allowing for evaporation on the wick surface only, providing short liquid return paths, and orienting the magnetic field parallel to the liquid metal flow.

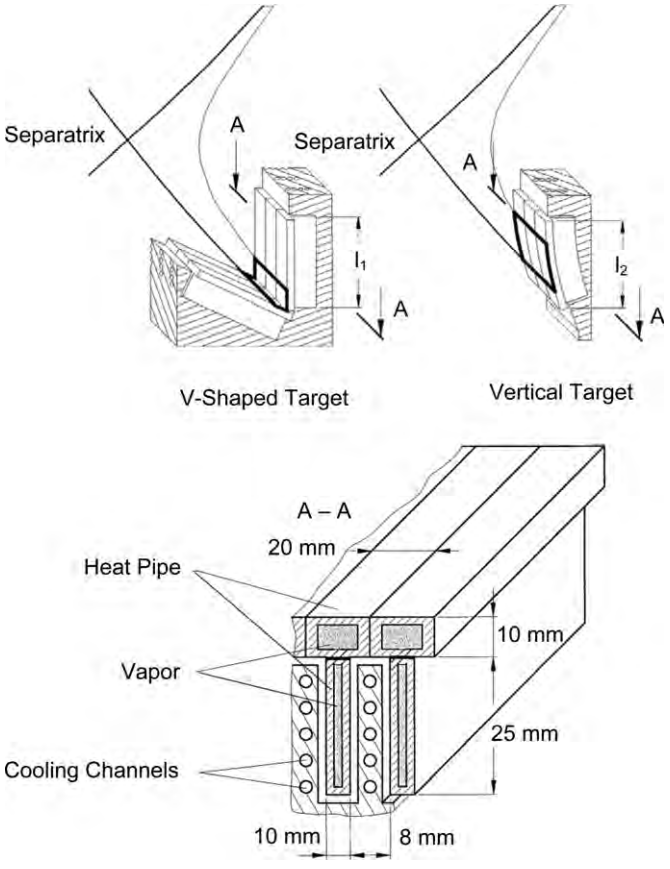

Fig. 21. Heat pipes for cooling V-shaped and vertical targets of the divertor employ sodium at 700 °C or lithium at 1000 °C as the working fluids, and V or W as the structural materials. Wick of the evaporation zone is made of Nb alloy felt and of the condensation zone of Nb or Mo perforated screens (Makhankov et al., 1998). ©1998 Elsevier, reproduced with permission.

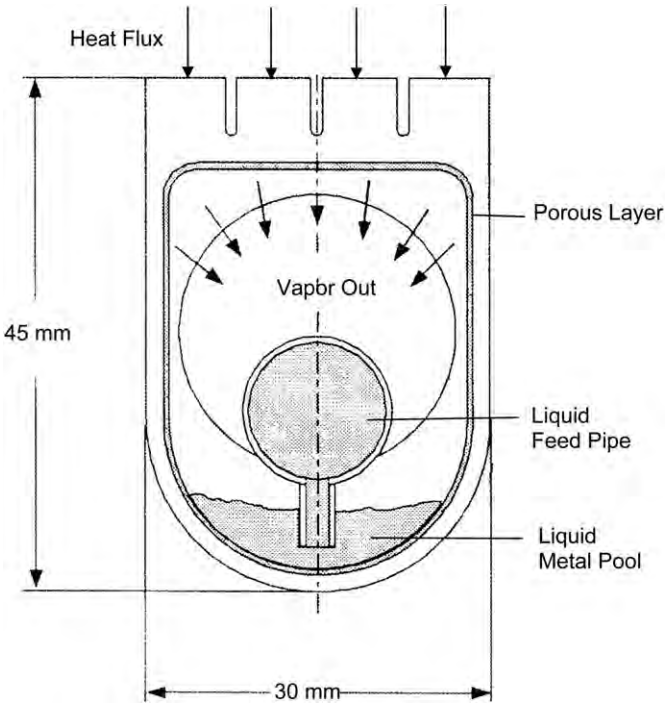

Fig. 22. A porous layer design concept employing Na or Li as the heat pipe working fluids. This configuration can handle heating loads up to 5 MW/m^2 (Reimann et al., 2001). No experimental test of this concept is available. © 2001 Elsevier, reproduced with permission.

Thermosyphons are even simpler heat transfer devices than heat pipes, because they employ only the working fluids (no wicks) to transfer heat between the evaporator and condenser sections of the pipes (Dobran, 1985; Reay and Kew, 2006). Such devices offer high simplicity and reliability, but do not appear to have been considered for removing heat from fusion reactors.

4. Conclusion

The development of viable fusion energy technology crucially depends on the effective heat removal from the reactor. The important energy conversion issues in magnetically confined plasma fusion reactors are associated with the first wall and divertor targets, where both the steady-state and the plasma disruption heating loads will have to be accommodated, and with the blankets and divertors from where the absorbed fusion energy will have to be removed. The tritium fuel for the reactor is envisaged to be produced within the blanket from either solid or liquid breeders, where the latter may also serve as the blanket coolants. In

steady-state most of the energy from plasma ions and impurities from plasma–wall interactions will be removed through the divertor. The plasma facing components of commercial fusion reactors will be exposed to large neutron and heat fluxes and potentially huge transient heat fluxes, requiring the development of advanced refractory metal alloys and ceramics for their protection. Advanced reduced-activation, tritium breeding, and coolant compatible materials will also have to be developed for blankets and divertors. ITER is an important first step where the conversion of fusion-to-thermal energy technology will be assessed, but it will not prove whether this technology is commercially viable. The operating conditions of this reactor are not as demanding on the materials, coolants, and tritium fuel production as those of the demonstration and more advanced commercial power reactors.

Several fusion reactor wall blanket and divertor energy conversion modules will be tested in ITER. Some of these test blanket modules involve high pressure helium gas as the principal first wall and blanket coolant, whereas the others involve combinations of helium, molten salts, and mixtures of lead and lithium as the blanket coolants. These modular energy conversion technologies are constrained by the materials, coolants, and tritium breeders. Some of the proposed advanced fusion energy removal concepts include liquid metal first walls, first walls made of jet-drop curtains, lithium flowing through the capillary pores of first walls, copper walls reinforced with ceramic fibres, liquid metals and molten salts flowing through the insulated channels of blankets, cooling of first walls and divertor targets with high pressure and velocity helium jets, evaporation of liquid metals within the heat pipes embedded into blankets and divertors, etc., but only some of these concepts have been tested under limited conditions. Most of these concepts have, however, one or more shortcomings, which will preclude their use in the next step fusion energy producing machines. This is because the next step demonstration and commercial fusion reactors will be operating with an order of magnitude higher neutron and heat loads and demand high reliability and long life of their energy conversion components.

We have not addressed in this paper the more technologically mature energy conversion systems associated with the fusion reactor support systems. These include cooling of superconducting magnets at about 4 K, cooling of the vacuum vessel, and processing of tritium and management of heat removed from the blankets and divertors on the outside of the vacuum vessel of the reactor. The DEMOs and subsequent commercial reactors operating at high thermal conversion efficiencies will necessarily require the development of advanced heat exchangers and gas turbine components.

Viable fusion energy producing machines should be simple, reliable, safe, efficient, and acceptable to the public, but these sustainability goals are difficult to achieve. Based on the past plasma confinement and materials development achievements we should, however, be optimistic that such machines can be built, before we run out of fossil fuels, fail to develop sustainable and alternative energy supply technologies, and produce an irreparable damage to the environment.

Acknowledgement

The author wishes to thank the anonymous reviewers whose comments improved the paper.

References

Abdou, M., 2007a. Overview of the principles and challenges of fusion nuclear technology.
Abdou, M., 2007b. Solid and liquid breeder blanket concepts.
Abdou, M., 2010. Scientific and engineering challenges and new strategy for development of practical fusion energy.
Abdou, M.A., The APEX Team, 2001. On the exploration of innovative concepts for fusion chamber technology. Fusion Engineering and Design 54, 181–247.
Abdou, M.A., Morley, N.B., Ying, A.Y., et al., 2005. Overview of fusion blanket R&D in the US over the last decade. Nuclear Engineering and Technology 37, 401–422.
Abdou, M.A., Morley, N.B., Ying, A.Y., et al., 2007. US ITER Test Blanket Module (TBM) Program. University of California Los Angeles Report UCLA-FNT-216.
Ahn, M.Y., Cho, S., Kim, D.H., et al., 2008. Preliminary safety analysis of Korea helium cooled solid breeder test blanket module. Fusion Engineering and Design 83, 1753–1758.
Akiba, M., Enoeda, M., Tanaka, S., 2010. Overview of the TBM R&D activities in Japan. Fusion Engineering and Design 85, 1766–1771. Tsuru, D., Tanigawa, H., Hirose, T., et al., 2008. Achievements of the water cooled solid breeder test blanket module of Japan to the milestones for installation in ITER. In: 22nd IAEA Fusion Energy Conference, Paper FT/P2-6, 13–18 October, Geneva.
Baluc, N., Abe, K., Boutard, J.L., et al., 2007. Status of R&D activities on materials for fusion power reactors. Nuclear Fusion 47, 696–717.
Barabash, V., The ITER International Team, 2007. Materials challenges for ITER – current status and future activities. Journal of Nuclear Materials 367-370, 21–32.
Baxi, C.B., 1995. Comparison of swirl tube and hypervapotron for cooling of ITER divertor. In: 16th IEEE/NPSS symposium on fusion engineering, vol. 1, 30 September–5 October, Champain, pp. 186–189.
Baxi, C.B., Wong, C.P.C., 1999. Review of Helium Cooling for Fusion Reactor Applications. General Atomics Report GA-A23181.
Blanchard, J.P., Raffray, R., 2007. Laser fusion chamber design. Fusion Science and Technology 52, 440–444.
Boccaccini, L.V., 2001. Design Description Document for the European Helium Cooled Pebble Bed (HCPB) Test Blanket Module. Forschungszentrum Karlsruhe Report FZKA.
Bolt, H., Roth, J., 2011. Plasma-facing materials and components (accessed 05.06.11). www.ipp.mpg.de/ippcms/de/for/projekte/pfmc/publikationen/2005.pdf.
Brendel, A., Popescu, C., Leyens, C., et al., 2004. SiC-fibre reinforced copper as heat sink material for fusion applications. Journal of Nuclear Materials 329-333, 804–808.
Bystrov, P.I., Kagan, D.N., Krechetova, G.A., Shpilrain, E.E., 1990. Liquid-metal Coolants for Heat Pipes and Power Plants. Hemisphere Publishing Corporation, New York.
Carlson, G.A., Hoffman, M.A., 1972. Heat pipes in the magnetic field environment of a fusion reactor. Journal of Heat Transfer 94, 282–288.
Chang, S.H., Baek, W.P., 2003. Understanding, predicting, and enhancing critical heat flux. In: 10th International Topical Meeting on Nuclear Reactor Thermal HYDRAULICS (NURETH-10), 5–9 October, Soul.
Chaudhuri, P., Danani, C., Chaudhari, V., et al., 2010. Current status of design and engineering analysis of Indian LLCB TBM. Fusion Engineering and Design 85, 1966–1969.
Cismondi, F., Kecskes, S., Ilic, M., et al., 2009. Design update, thermal and fluid dynamic analyses of the EU-HCPB TBM in vertical arrangement. Fusion Engineering and Design 84, 607–612.
DATASHEET – High Temperature Heat Pipes, 2008. Thermacore Inc. (accessed 1705.11). www.thermacore.com.
Davison, H.W., 1968. Compilation of Thermophysical Properties of Liquid Lithium. NASA TN D-4650, Washington D.C.
Dobran, F., 1985. Steady-state characteristics and stability thresholds of a closed two-phase thermosyphon. International Journal of Heat and Mass Transfer 28, 949–957.
Dobran, F., 1987. Super heat pipe design considerations for applications to space-based systems. In: Dobran, F., Imber, M. (Eds.), 1987. International Symposium on Thermal Problems in Space-Based Systems, vol. 83. ASME HTD, pp. 1–12.
Dobran, F., 1989. Heat pipe research and development in the Americas. Heat Recovery & CHIP 9, 67–100.
Dobran, F., 2010. Energy Supply Options for Climate Change Mitigation and Sustainable Development. In: XXI World Energy Congress. Curran Associates, Montreal. www.proceedings.cpm.
Dobran, F., 2011. Sustainability attributes and their implementation in energy resources utilization. In: ASME 2011 Fifth International Conference on Energy Sustainability, Paper ESFuelCell2011-54269, 7–10 August, Washington, D.C.
EFDA, 2005. A Conceptual Study of Commercial Fusion Power Plants. European Fusion Development Agreement Report EFDA-RP-RE-5.0. (accessed 22.03.11).
EIA, 2010. International Energy Outlook 2010. U.S. Energy Information Administration. www.eia.doe.gov/oiaf/ieo.
Escourbiac, F., 2008. High heat flux and critical heat flux (CHF) tests in support to ITER HHFC. In: International HHFC Workshop, 10–12 December, San Diego.
Escourbiac, F., Bobin-Vastra, I., Kuznetsov, V., et al., 2005. A mature industrial solution for ITER divertor plasma facing components: Hypervapotron cooling concept adapted to Tore Supra flat tile technology. Fusion Engineering and Design 75-79, 387–390.
EUP. 2003. Thermonuclear Fusion. European Parliament Report STOA 114 EN.
Evtikhin, V.A., Lyublinski, I.E., Vertkov, A.V., et al., 2000. Energy removal and MHD performance of lithium capillary-pore systems for divertor target application. Fusion Engineering and Design 49-50, 195–199.
Farmer, J.C., 2008. LIFE Materials: Overview of Fuels and Structural Materials Issues, vol. 1. Lawrence Livermore National Laboratory Report LLNL-TR-407386-Rev.1.
Federici, G., Skinner, C.H., Brooks, J.N., et al., 2001. Plasma-material interactions in current tokamaks and their implications for next step fusion reactors. Nuclear Fusion 41, 1967–2137.
Federici, G., Wuerz, H., Janeschitz, G., Tivey, R., 2002. Erosion of plasma-facing components in ITER. Fusion Engineering and Design 61-62, 81–94.

Feng, K.M., Pan, C.H., Zhang, G.S., et al., 2008. Overview of design and R&D of solid breeder TBM in China. In: 22nd IAEA Fusion Energy Conference, Paper FT/P2-9, 13–18 October, Geneva; Feng, K.M., Pan, C.H., Zhang, G.S., et al., 2010. Progress in solid breeder TBM at SWIP. Fusion Engineering and Design 85, 2132–2140.

Fukuda, G.T., Peterson, P.F., Olander, D.R., Prausnitz, J.M., 2007. Thermodynamics of the LiF–NaF–BeF_2 system at high temperatures. Fluid Phase Equilibria 255, 1–10.

Gasparotto, M., 2009. ITER: Status of the project. Presentation 27 May 2009, Barcelona. http://fusionforenergy.europa.eu/uploads/documents/090527_ev_info/InfodayPS1-Overview-of-the-ITER-project-Gasparotto.pdf (accessed 24.03.11). See also: Holtkamp, N., 2007. An overview of the ITER project. Fusion Engineering and Design 82, 427–434.

Gierszewski, P., Mikic, B., Todreas, N., 1980. Property Correlations for Lithium, Sodium, Helium, Flibe and Water in Fusion Reactor Applications. MIT Report PFC-RR-80-12.

Golubchikov, L.G., Evtikhin, V.A., Lyblinski, I.E., et al., 1996. Development of a liquid-metal fusion reactor divertor with a capillary-pore system. Journal of Nuclear Materials 233-237, 667–672.

Gomes, R.B., Fernandes, H., Silva, C., et al., 2008. Interaction of a liquid gallium jet with the tokamak ISTTOK edge plasma. Fusion Engineering and Design 83, 102–111.

Gross, R.A., 1984. Fusion Energy. John Wiley & Sons, New York.

Harms, A.A., Schoepf, K.F., Miley, G.H., Kingdon, D.R., 2000. Principles of Fusion Energy. World Scientific, Singapore.

Hermsmeyer, S., Malang, S., 2002. Gas-cooled high performance divertor for a power plant. Fusion Engineering and Design 61-62, 197–202.

Herrmann, A., Greuner, H., Balden, M., Bolt, H., 2011. Design and evaluation of an optimized W/Cu interlayer for W monoblock components. Fusion Engineering and Design 86, 27–32.

IAEA, 1995. Energy from Inertial Fusion. International Atomic Energy Agency, Vienna.

IAEA, 2009. Molten Salt Coolants for High Temperature Reactors. IAEA Internship Report NENP-TDS/INPRO.

Ibbot, C., Chiocchio, S., D'Agata, E., et al., 2001. Overview of the engineering design of ITER divertor. Fusion Engineering and Design 56-57, 243–248.

Ihli, T., Ilić, M., 2009. Efficient helium cooling methods for nuclear fusion devices. Fusion Engineering and Design 84, 964–968.

Ihli, T., Raffray, A.R., Abdel-Khalik, S.I., Shin, S., 2007. Design and performance study of the helium-cooled T-tube divertor concept. Fusion Engineering and Design 82, 249–264.

IPCC, 2007a. Climate Change 2007: The Physical Science Basis. Solomon, S., Qin, D., Manning, M., Chen, Z., Marquis, M., Averyt, K.B., Tignor, M., Miller, H.L. (Eds.), Contribution of Working Group I to the Fourth Assessment Report of the Intergovernmental Panel on Climate Change. Cambridge University Press, Cambridge. www.ipcc.ch.

IPCC, 2007b. Climate Change 2007: Mitigation of Climate Change. Metz, B., Davidson, O.R., Bosch, P.R., Dave, R., Meyer, L.A. (Eds.), Contribution of Working Group III to the Fourth Assessment Report of the Intergovernmental Panel on Climate Change. Cambridge University Press, Cambridge. www.ipcc.ch.

ITER, 2001. Summary of the ITER Final Design Report G A0 FDR 4 01-06-28 R 0.2 (accessed 04.04.11). http://fire.pppl.gov/iter_summary_FDR2001.pdf.

ITER, 2002. ITER Technical Basis: ITER EDA Documentation Series No. 24. International Atomic Energy Agency, Vienna. ITER website. http://www.iter.org.

Klimiankou, M., Lindau, R., Moslang, A., 2003. HRTEM study of yttrium oxide particles in ODS steels for fusion reactor applications. Journal of Crystal Growth 249, 381–387.

Končar, B., Simonovski, I., Draksler, M., 2011. Influence of multiple jet cooling on the heat transfer and thermal stresses in DEMO divertor cooling finger. Fusion Engineering and Design 86, 167–173.

Kovalenko, V., Khripunov, V., Antipenkov, A., Ulianov, A., 1995. Heat-pipes-based first wall. Fusion Engineering and Design 27, 544–549.

Linke, J., 2006. High heat flux performance of plasma facing materials and components under service conditions on future fusion reactors. Fusion Science and Technology 49, 455–464.

Lyublinski, I.E., Vertkov, A.V., Evtikhin, V.A., et al., 2010. Development and experimental study of lithium based plasma facing elements for fusion reactor applications. In: 23rd IAEA Fusion Energy Conference, Paper FTP/3-6Rb, 11–16 October, Daejeon.

Maisonnier, D., 2008. European DEMO design and maintenance strategy. Fusion Engineering and Design 83, 858–864.

Majeski, R., 2010. Liquid Metal Walls, Lithium, and Low Recycling Boundary Conditions in Tokamaks. Princeton Plasma Physics Laboratory Report PPPL-4480.

Majeski, R., Berzak, L., Doerner, R., 2010. First results from the lithium tokamak eXperiment (LTX). In: 23rd IAEA Fusion Energy Conference, 11–16 October, Daejeon.

Makhankov, A., Anisimov, A., Arakelov, A., et al., 1998. Liquid metal heat pipes for fusion application. Fusion Engineering and Design 42, 373–379.

Milnes, J., 2010. Computational Modelling of the HyperVapotron Cooling Technique For Nuclear Fusion Applications. Ph.D. thesis, Department of Aerospace Sciences, Cranfield University, Cranfield, UK.

Mirnov, S., 2009. Plasma-wall interactions and plasma behaviour in fusion devices with liquid lithium plasma facing components. Journal of Nuclear Materials 390-391, 876–885.

Mirnov, S.V., Evtikhin, V.A., 2006. The tests of liquid metals (Ga, Li) as plasma facing components in T-3M and T-11M tokamaks. Fusion Engineering and Design 81, 113–119.

Mistrangelo, C., Bühler, L., 2009. Influence of helium cooling channels on magnetohydrodynamic flows in the HCLL blanket. Fusion Engineering and Design 84, 1323–1328.

Mitteau, R., Stangeby, P., Lowry, C., Merola, M., 2010. Heat loads and shape design of the ITER first wall. Fusion Engineering and Design 85, 2049–2053.

Morley, N.B., Abdou, M.A., Anderson, M., et al., 2006. Overview of fusion nuclear technology in the US. Fusion Engineering and Design 81, 33–43.

Najmabadi, F., The ARIES Team, 2006. The ARIES-AT advanced tokamak, advanced technology fusion power plant. Fusion Engineering and Design 80, 3–23 (See also other articles in this ARIES-AT Special Issue of the journal).

Nakamura, H., Ida, M., Nakamura, H., et al., 2003. Liquid lithium target under steady state ultra high heat load of 1 GM/m^2 range for International Fusion Materials Irradiation Facility (IFMIF). Fusion Engineering and Design 65, 467–474.

NAP, 2003. Burning Plasma: Bringing a Star to Earth. National Academies Press, Washington D.C.

Narula, M., Abdou, M.A., Ying, A., et al., 2006. Exploring liquid metal plasma facing component (PFC) concepts – liquid metal film flow behavior under fusion relevant magnetic fields. Fusion Engineering and Design 81, 1543–1548.

National Ignition Facility. https://lasers.llnl.gov.

Noda, T., 1999. Boronization in future devices – protecting layer against tritium and energetic neutrals. Journal of Nuclear Materials 266-269, 234–239.

Norajitra, P., Bühler, L., Buenaventura, A., et al., 2003. Conceptual design of the EU dual-coolant blanket (Model C). In: 20th IEEE/NPSS Symposium on Fusion Engineering Paper IV. 14–17 October, San Diego; Norajitra, P., Bühler, L., Fisher, U., et al., 2003. Conceptual design of the dual-coolant blanket in the frame of the EU power plant conceptual study. Fusion Engineering and Design 69, 669–673.

Norajitra, P., Giniyatulin, R., Ihli, T., et al., 2005. European development of He-cooled divertors for fusion power plants. Nuclear Fusion 45, 1271–1276.

Norajitra, P., Giniyatulin, R., Kuznetsov, V., et al., 2010. He-cooled divertor for DEMO: Status of development and HHF tests. Fusion Engineering and Design 85, 2251–2256.

Nygren, R.E., Rognlien, T.D., Rensink, M.E., et al., 2003. Liquid surface divertor designs for fusion reactors. In: 20th Symposium on Fusion Engineering, Paper UCRL-PROC-200896, 14-17 October, San Diego. See also: Nygren, R.E., Rognlien, T.D., Rensink, M.E., et al., 2004. A fusion reactor design with a liquid first wall and divertor. Fusion Engineering and Design 72, 181–221.

Nygren, R.E., Raffray, R., Whyte, D., et al., 2011. Making tungsten work. Journal of Nuclear Materials 417, 451–456.

Olson, C., Rochau, G., Slutz, S., et al., 2005. Development path for Z-pinch IFE. Fusion Science and Technology 47, 633–640.

Ongena, J., Van Oost, G., 2006. Energy for future centuries. Fusion Science and Technology 49, 3–15.

Philipps, V., 2004. Plasma wall interaction and its control by wall conditioning. Fusion Science and Technology 45, 237–248.

Pitts, R.A., Carpentier, S., Escourbiac, F., et al., 2011. Physics basis and design of ITER plasma-facing components. Journal of Nuclear Materials 415, S957–S964.

Poitevin, Y., Boccaccini, L.V., Zmitko, M., et al., 2010. Tritium breeder blankets design and technologies in Europe: Development status of ITER test blanket module, test & qualification strategy and roadmap towards DEMO. Fusion Engineering and Design 85, 2340–2347.

Pulsifer, J.E., Raffray, A.R., 2002. Structured porous media for high heat flux fusion applications. In: 19th IEEE/NPSS Symposium on Fusion Engineering, Atlantic City.

Raffray, A.R., El-Guebaly, L., Sze, D.K., et al., 1999a. SiC/SiC composite for an advanced fusion power plant blanket. Fusion Engineering, 73–76.

Raffray, A.R., Schlosser, J., Akiba, M., et al., 1999b . Critical heat flux analysis and R&D for the design of the ITER divertor. Fusion Engineering and Design 45, 377–407.

Raffray, A.R., Pulsifer, J.E., Tillack, M.S., 2002. Advanced Heat Sink Material for Fusion Energy Devices. University of California San Diego Report UCSD-ENG-107.

Raffray, A.R., Nygren, R., Whyte, D.G., et al., 2010. High heat flux components – readiness to proceed from near term fusion systems to power plants. Fusion Engineering and Design 85, 93–108.

Reay, D., Kew, P., 2006. Heat Pipes: Theory, Design and Applications. Butterworth-Heinemann, Oxford.

Reimann, J., Barleon, L., Boccaccini, L., Malang, S., 2001. Conceptual design of an evaporation-cooled liquid metal divertor for fusion power plants. Fusion Engineering and Design 56-57, 369–373.

Roth, J., Tsitrone, E., Loarte, A., et al., 2009. Recent analysis of key plasma wall interactions issues for ITER. Journal of Nuclear Materials 390-191, 1–9.

Salavy, J.-F., Aiello, G., David, O., et al., 2008. The HCLL test blanket module system: Present reference design, system Integration in ITER and R&D needs. Fusion Engineering and Design 83, 1157–1162.

Samuel, D., May 2009. Molten Salt Coolants for High Temperature Reactors. IAEA Internship Report INPRO COOL.

Santarius, J.F., Kulcinski, G.L., El-Guebaly, L.A., Khater, H.Y., 1998. Could Advanced Fuels be Used with Today's Technology? Fusion Technology Institute, University of Wisconsin Report UWFDM-1062.

Sawan, M.E., Youssef, M.Z., 2006. Three-dimensional neutronics assessment of dual coolant molten salt blankets with comparison to one-dimensional results. Fusion Engineering and Design 81, 505–511.

Sharafat, S., Ghoniem, N., 2000. Summary of Thermo-physical Properties of Sn, and Compounds of Sn-H, Sn-O, Sn-C, Sn-Li, and Sn-Si and Comparison of Properties of Sn, Sn–Li, Li, and Pb–Li. University of California UCLA-UCMEP-00-31 Report.

Sharafat, S., Mills, A., Youchison, D., et al., 2007. Ultra low pressure-drop helium-cooled porous-tungsten PFC. Fusion Science and Technology 52, 559–565.
Shimada, M., Cambell, D.J., Mukhovator, V., et al., 2007. Chapter 1: overview and summary. Nuclear Fusion 47, S1–S17.
Smith, C.L., Ward, D., 2007. The path to fusion power. Philosophical Transactions of the Royal Society A 365, 945–956.
Smolentsev, S., Moreau, R., Bühler, L., Mistrangelo, C., 2010. MHD thermofluid issues of liquid metal blankets: Phenomena and advances. Fusion Engineering and Design 85, 1196–1205.
Stacey, W.M., 2010. Fusion: An Introduction to the Physics and Technology of Magnetic Confinement Fusion. Wiley-Vch Verlag GmbH & Co, KGaA, Weinheim.
Suri, A.K., Krishnamurthy, N., Batra, I.S., 2010. Materials issues in fusion reactors. Journal of Physics: Conference Series 2008, 012001. 1–16.
Sze, D.K., Hassanein, A., 1993. Design windows for a He cooled fusion reactor. Fusion Engineering 1, 169–172.
Terai, T., 2001. Advanced blanket concepts and their R&D issues. In: Katoh, Y. (Ed.), Introduction to Fusion Engineering. Atomic Energy Society of Japan, p. 123.
Tillack, M.S., Wang, I.P., Pulsifer, J., et al., 2003. Fusion power core engineering for the ARIES-ST power plant. Fusion Engineering and Design 65, 215–261.
Tillack, M.S., Raffray, A.R., Wang, X.R., et al., 2011. Recent US activities on advanced He-cooled W-alloy divertor concepts for fusion power plants. Fusion Engineering and Design 86, 71–98.
Tobita, K., Utoh, H., Someya, Y., et al., 2010. Concept of power core components of the SlimCS Fusion DEMO reactor. In: 23nd IAEA Fusion Energy Conference, Paper FTP/P6–20, 11–16 October, Daejan.
Ueda, Y., 2008. Status of plasma facing material studies and issues toward DEMO. In: 18th International Toki Conference, 9–12 December, Toki, Japan.
UNDESA, 2008. World Population to 2300. United Nations Department of Economic and Social Affairs Report ST/ESA/SER.A/236.
U.S. ARIES, APEX, FIRE Joint European Torus; Willis, J., 2005. Bringing a star to Earth. Presentation January 24, 2005 (accessed 04.04.11).
Valanju, P.M., Kotschenreuther, M., Mahajan, S.M., 2010. Super X divertors for solving heat and neutron flux problems of fusion devices. Fusion Engineering and Design 85, 46–52.
Vergaftik, N.B., 1975. Tables on the Thermophysical Properties of Liquids and Gases. Hemisphere, New York.
Vertkov, A., Lyublinski, I., Evtikhin, V., et al., 2007. Technological aspects of liquid lithium limiter experiment on FTU tokamak. Fusion Engineering and Design 82, 1627–1633.
Werner, R.W., Hoffman, M.A., 19 July 1983. Heat pipes for use in a magnetic field. United States Patent 4,394,344.
Williams, D.F., Toth, L.M., Clarno, K.T., 2006. Assessment of Candidate Molten Salt Coolants for the Advanced High-Temperature Reactor (AHTR). Oak Ridge National Laboratory Report ORNL/TM-2006/12.
Wong, C.P.C., 2009. Innovative tokamak DEMO first wall and divertor material concepts. Journal of Nuclear Materials 390–391, 1026–1028.
Wong, C.P.C., Baxi, C.B., Hamilton, et al., 1994. Helium-cooling in Fusion Power Plants. General Atomics Report GA-A21804.
Yang, Z., Zhou, T., Chen, H., Ni, M., et al., 2010. Numerical study of MHD pressure drop in rectangular ducts with insulating coatings. Fusion Engineering and Design 85, 2059–2064.
Youchison, D.L., North, M.T., 2001. Thermal performance of a dual-channel, helium-cooled, tungsten heat exchanger. Fusion Technology 39, 899–904.
Youchison, D.L., Lutz, T.J., Williams, B., Nygren, R.E., 2007. High heat flux testing of a helium-cooled tungsten tube with porous foam. Fusion Engineering and Design 82, 1854–1860.
Zaghloul, M.R., Sze, D.K., Raffray, A.R., 2003. Thermo-physical properties and equilibrium vapor composition of lithium fluoride-beryllium fluoride (2LiF/BeF2) molten salt. Fusion Science and Technology 44, 344–350.
Zhang, X., Xu, A., Pan, C., 2010. Numerical analysis of MHD duct flow with a flow channel insert. Fusion Engineering and Design 85, 2090–2094.
Zinkle, S.J., 2005a. Advanced materials for fusion technology. Fusion Engineering and Design 74, 31–40.
Zinkle, S.J., 2005b. Fusion materials science: Overview of challenges and recent progress. Physics of Plasmas 12, 058101–1–8.
Zinkle, S.J., Ghoniem, N.M., 2000. Operating temperature windows for fusion reactor structural materials. Fusion Engineering and Design 51-52, 55–71.
Zinkle, S., 27–28 July 1998. Summary of Physical Properties for Li, Pb-17Li, and $(LiF)_n \cdot BeF_2$ Coolants. In: APEX Study Meeting. Sandia National Laboratory.